

Copy 9
SL53G09c

70151

65-86405

NACA

RESEARCH MEMORANDUM

for the

Atomic Energy Commission

AN INVESTIGATION OF THE DYNAMIC AND STATIC STABILITY
CHARACTERISTICS OF A GROUP OF SPECIALIZED STORE
CONFIGURATIONS AT TRANSONIC SPEEDS

By Beverly Z. Henry, Jr., and John A. Braden

Langley Aeronautical Laboratory
Langley Field, Va.

CONCLUSIONS

NATIONAL ADVISORY COMMITTEE
FOR AERONAUTICS

WASHINGTON

AUG 21 1953

Declassified by authority of NASA
Classification Change Notices No. 1
Dated 11-5-54

Authorizing: Executive Order 12812
Authority: P.O. Proclamation 4380-1
Accession: 3-25-65; 12812-5197

5/97



SECRET

NOV 63

NACA RM SL53G09c

SECURITY INFORMATION

NATIONAL ADVISORY COMMITTEE FOR AERONAUTICS

RESEARCH MEMORANDUM

for the

Atomic Energy Commission

AN INVESTIGATION OF THE DYNAMIC AND STATIC STABILITY
CHARACTERISTICS OF A GROUP OF SPECIALIZED STORE
CONFIGURATIONS AT TRANSONIC SPEEDS

By Beverly Z. Henry, Jr., and John A. Braden

SUMMARY

An investigation was conducted in the Langley 8-foot transonic tunnel to determine the dynamic and static stability characteristics of the Mark-6, Mark-4, TX-4, TX-13, and Mark-5 special weapons and the effects of modifications thereto in the Mach number range from 0.70 to 1.10. The Reynolds numbers for these tests varied from approximately 2.15×10^6 to 2.5×10^6 . Because of the highly specialized nature of these configurations a complete analysis of the stability characteristics has not been made.

In all cases investigated the Mark-6 displayed a region of dynamic instability in the Mach number range between about 0.84 to 0.86 and 0.92 to 0.94 and a small region of low-amplitude static instability near a Mach number of 0.97. The addition of artificial roughness, suspension lugs, or fin-mounted fan ducts to the Mark-6 resulted in no appreciable change in the stability characteristics. Reducing the Reynolds number of the Mark-6 from 2.5×10^6 to 2.15×10^6 lowered the Mach numbers at which sudden changes in dynamic stability occurred but had no appreciable effect on static stability. A rearward movement of the center of gravity reduced the dynamic stability and increased the region of dynamic instability. The use of 4° - 20° fins resulted in a small decrease in the Mach number range of dynamic instability but this decrease was accompanied by an increased region of static instability near a Mach number of 1.0.

The Mark-4 configuration exhibited an increase in dynamic stability at low Mach numbers over that of the Mark-6 and a reduction at higher Mach numbers, with the region of dynamic instability occurring at higher Mach numbers. The static stability for the Mark-4 was generally lower than that for the Mark-6 at Mach numbers below 0.95, above which the reverse was true.

Declassified by authority of NASA
Classification Change Notices No. 16-1
Dated 11/15/85

DECLASSIFIED

The TX-4 configuration exhibited no unstable characteristics, either dynamic or static, throughout the Mach number range of this investigation.

In all cases the TX-13B¹ exhibited a region of static instability in the Mach number range from about 0.95 to 0.99. Changes in center-of-gravity location resulted in no discernible change in this phenomena. The region of static instability was not exhibited by the TX-13C although a general decrease in dynamic stability was noted at the higher Mach numbers with a small region of neutral stability occurring near a Mach number of 0.92.

The Mark-5 configuration exhibited no unstable characteristics, either dynamic or static, throughout the Mach number range of the tests. Rapid variations of dynamic stability with Mach number were noted in the range of Mach numbers from about 0.85 to 1.0.

While certain effects of Reynolds number were noted, these and other similar investigations have indicated the existence of Reynolds number effects which are not clearly defined by the presently available information. Until such time as these effects are defined, care should be exercised in the extrapolation of wind-tunnel results to full-scale conditions.

In general the configurations which exhibited the more desirable performance characteristics were those which were less subject to a highly complex or separated flow. Improvements in the local flow conditions would therefore be expected to have an advantageous effect on the stability performance of these bodies.

INTRODUCTION

In the foreseeable future aircraft will become operational which are capable of releasing special weapons from altitudes above fifty thousand feet at high subsonic Mach numbers. Under these release conditions the weapons will attain supersonic speeds during their descent. Available wind-tunnel data concerning the longitudinal stability characteristics of these specialized shapes has been limited to subsonic Mach numbers below 0.97 and at a supersonic Mach number of 1.2. The need for determining the longitudinal stability characteristics of these weapons in the Mach number range near the speed of sound was apparent.

In accordance with the request of the Atomic Energy Commission and in cooperation with the Sandia Corporation in the development of satisfactory store configurations, tests were conducted in the Langley 8-foot transonic tunnel of the Mark-6, Mark-4, TX-4, TX-13, and Mark-5 special weapons. The investigation covered the Mach number range from 0.7 to

approximately 1.10. Due to the highly specialized nature of the special weapons program and to the relatively limited amount of information obtained from this investigation, any complete evaluation of these weapons is beyond the scope of this paper.

SYMBOLS

M_0	free-stream Mach number
V_0	free-stream velocity, ft/sec
ρ_0	free-stream density, slugs/cu ft
d	maximum body diameter, ft
S	body frontal area, sq ft
R	Reynolds number, based on d
I	transverse moment of inertia of the body about its center of gravity, slug-ft ²
$T_{1/2}$	time to damp to half amplitude for a decaying motion, sec
T_2	time to increase to double amplitude for a divergent motion, sec
P	period of oscillation, sec
α	angle of attack, radians or degrees
q	pitching velocity, radians/sec
C_{m_q}	effective rate of change of pitching-moment-curve slope with reduced pitching velocity, $\left. \frac{\partial C_m}{\partial \left(\frac{qd}{2V} \right)} \right _{q \rightarrow 0}$
$C_{m_{\dot{\alpha}}}$	effective rate of change of pitching-moment-curve slope with reduced rate of change of angle of attack, $\left. \frac{\partial C_m}{\partial \left(\frac{\dot{\alpha} d}{2V} \right)} \right _{\dot{\alpha} \rightarrow 0}$
$C_{m_q} + C_{m_{\dot{\alpha}}}$	rotational damping coefficient, per radian
$C_{m_{\alpha}}$	static-longitudinal-stability parameter, $\partial C_m / \partial \alpha$, per degree

DECLASSIFIED

MODEL DESCRIPTION

The models tested in this investigation and provided by the Sandia Corporation consisted of five primary configurations designated as the Mark-6, Mark-4, TX-4, TX-13, and Mark-5. Drawings of these configurations are presented in figure 1. The bodies of these basic configurations were obtained through combinations of three forebody and three afterbody shapes and by addition to the noses and afterbodies of spoiler bands, suspension lugs, and a cylindrical extension at the body midsection.

The models were constructed principally of magnesium and utilized cruciform, wedge-type stabilizing fins attached to the afterbody section at an angle of 45° from the vertical plane. The maximum diameters of the bodies were 6.5 and 7.5 inches and represented the full-size missiles to 0.1083 and 0.1250 scales, respectively. With exceptions of the TX-13 and Mark-5 designs, the fineness ratio of all the models was about 2.1. The fineness ratios for the TX-13 configurations, in which a 0.284d cylindrical midbody extension was used, and for the Mark-5 were, respectively, about 2.4 and 2.9.

A nomenclature of the model components has been previously devised and is used herein. Each model configuration is denoted by a series of letters, each letter being assigned to a component part or characteristic of the model assembly. The letter is followed by a subscript representing a full-scale dimension or is descriptive of the full-scale counterpart, and a superscript referring to a model dimension. The following table lists the model components and their designations:

$N_{40}^{6.5}$	Mark-4 nose, maximum diameter 6.5 in. (model scale)
$N_{40}^{7.5}$	Mark-4 nose, maximum diameter 7.5 in.
$N_{50}^{7.5}$	elliptical nose, maximum diameter 7.5 in.
$N_{54}^{6.5}$	Mark-5 nose, maximum diameter 6.5 in.
E_{17}	cylindrical extension at the body midsection - 17 inches long, full-scale
B_{40}	Mark-4 afterbody
B_{TX-4}	basic TX-4 afterbody

B ₅₄	basic Mark-5 afterbody
G _X	center-of-gravity position, the subscript representing the full-scale distance from the nose flat to the center of gravity
R ^{NF} ₂₈₀	artificial roughness. Superscripts refer to roughness on nose, N, and on fins, F. Subscript refers to type of roughness - No. 280-mesh carborundum grit.
S _E	Mark-6 spoiler-band arrangement
S ₃₆₇₈₉	TX-13B' spoiler-band arrangement
F ₅₋₂₅	Standard Mark-4, 5°-25° double-wedge fin
F ^S ₅₋₂₅ D ¹⁻³	full-length fin-fan duct on a shortened F ₅₋₂₅ fin. The superscripts (i.e., 1-3) refer to the fin position where ducts were mounted
F ₄₋₂₀	Standard Mark-4, 4°-20° double-wedge fin
F ₁₂	TX-4, 12° single-wedge fin
F ₁₆	Standard Mark-5, 16°-0° slab-sided fin
t	Standard Mark-5, fin tab
l ^{XX}	suspension lug, superscripts denoting lug positions

A prefix number with fin designations refers to the number of a given type used. If prefix is omitted, four fins of the same type were installed.

The above system has been utilized to index in table I the combinations of forebodies, afterbodies, and accessories used to obtain the primary and modified test configurations. It should be noted that the Mark-6 and the TX-13B' were tested as both 7.5- and 6.5-inch maximum-diameter bodies. Coordinates for the forebody and afterbody shapes are given in table II.

The wedge-type stabilizing fins (fig. 2) were of magnesium with the exception of the 4°-20° double-wedge fins (fig. 2(d)), which were of brass. The simulated ducted windmill generator or fin fan duct (fig. 2(c)) was adapted to a shortened 5°-25° double-wedge fin, the short fin keeping the installation within the limits of the maximum body diameter.

Spoiler bands and suspension lugs, shown in figure 3, were of steel and were screw-fastened to the body surfaces. Artificial roughness strips of No. 280-mesh carborundum grit were applied to the noses and fins with a commercial plastic spray.

A cut-away drawing of a typical model installation on the dynamic sting assembly is given in figure 4. The nose and afterbody sections were screw-fastened to the yoke of the dynamic rig and were statically balanced about the model pitch axis by means of lead or brass counterweights. Changes in center-of-gravity location were made by shifting the model longitudinally on the yoke. The models were actuated and controlled by the hydraulic pistons in which a fluid pressure of about 600 pounds per square inch was used. The attitude of the model was determined from the output of the strain-gage beam.

TESTS AND METHODS

Wind tunnel.- This investigation was conducted in the Langley 8-foot transonic tunnel which has a dodecagonal, slotted test section and permits continuous testing up to a Mach number of approximately 1.10 for these models. Details of the test section are reported in reference 1. Aerodynamic properties of the airstream are given in reference 2 wherein it is shown that the flow angularity in the test section is about 0.1° upflow and the maximum deviation from the indicated free-stream Mach number is ± 0.003 . For this investigation the indicated order of magnitude of the stream fluctuation was approximately $\pm 0.3^\circ$.

A sketch of the general arrangement of a typical sting-mounted model configuration in the test section is given in figure 5 and photographic views of typical models are shown in figure 6. For all the tests, the nose of the model was located in the test section approximately 80 inches downstream of the slot origin as shown in figure 5. Additional sting rigidity was obtained through the use of four 1/16-inch-diameter steel guy wires also shown in the figure.

The investigation was conducted through the Mach number range from 0.7 to approximately 1.10. The Reynolds number variation, presented in figure 7, was from 2.15×10^6 to 2.5×10^6 depending on the size of the model used.

The natural frequency of the system, with the sting support secured by guy wires was approximately 22 cycles per second. This value is considerably in excess of the model frequencies. Stresses at the intersection of the cylindrical and conical portions of the sting support were monitored continuously by means of electrical strain gages attached

at this point. The results of this monitoring indicated a negligible deflection of the support system under all loading conditions encountered during the investigation.

Considerable foreign matter carried by the airstream resulted in rather severe pitting of the model forebodies which were constructed of an extremely soft material. As a consequence the validity of comparisons between the smooth models and the models with artificial roughness applied may be somewhat questionable.

At each test point where dynamic stability existed the model was deflected from a trim position to an angle of attack of approximately 4° and locked in this deflected position. The model was then released and allowed to oscillate with one degree of freedom. In cases where dynamic instability existed the divergent motion was obtained by releasing the brake mechanism and allowing the model to oscillate. Three successive records of the model motion were obtained on each of two recording instruments. One instrument was a photographically recording galvanometer and the other a direct inking oscillograph.

Flow visualization in the vicinity of the models was obtained by the use of standard schlieren photographs and high-speed (930 frames per second) schlieren motion pictures.

All pressure data relative to the prevailing ambient test conditions were photographically recorded from multiple-tube manometers and tunnel total temperatures were obtained from a recording potentiometer.

REDUCTION OF DATA

Reduction of the data to determine the rotational damping coefficient, $C_{m_q} + C_{m_{\dot{\alpha}}}$, and the static longitudinal stability parameter, $C_{m_{\alpha}}$, was carried out according to the methods presented in reference 3, in which the following relationships were shown to exist:

$$-(C_{m_q} + C_{m_{\dot{\alpha}}}) = \frac{1.386}{T_{1/2}} \left(\frac{4I}{\rho_o V_o S d^2} \right)$$

$$(C_{m_q} + C_{m_{\dot{\alpha}}}) = \frac{1.386}{T_2} \left(\frac{4I}{\rho_o V_o S d^2} \right)$$

$$-C_{m\alpha} = \frac{1.755I/d^3}{P^2\rho_o V_o^2}$$

The time to damp to one-half amplitude, $T_{1/2}$, or the time to double amplitude, T_2 , and the period of the model motion, P , were evaluated at each test point by averaging three successive oscillograph records from the recording galvanometer. In the Mach number regions where a diverging motion occurs, only a few indicative points have been reduced, primarily because of a lack of an accurate method of determining whether the model was oscillating freely or striking the brake as it was retracted. The model moments of inertia, given in table I, were determined through the use of a calibrated, torsional pendulum. Static position calibrations to determine the variation of the strain-gage output with angle of attack were made at frequent intervals. The variation of gage output with angle of attack was considered sufficiently linear to permit the construction of the damping envelopes directly from the oscillograph records.

In the interests of consistency, since the damping rate was nonlinear with amplitude, the damping envelopes were constructed with the amplitude for the initial time as near $\pm 4^\circ$ as possible. Since the oscillatory motion of these models was mechanically restricted to approximately $\pm 4^\circ$, it should be noted that motions which appear as dynamic instability for these tests could conceivably represent a condition of neutral stability of amplitude slightly greater than $\pm 4^\circ$.

ACCURACY OF DATA

The largest error involved in the computation of $C_{m_q} + C_{m_{\dot{\alpha}}}$ was the non-repeatability of the damping envelopes for the three successive records. Maximum deviations from the mean value of the time to damp to one-half amplitude were found to vary from about 0 to 50 percent even in apparently stable Mach number regions. In those cases where the deviations from the mean were large and the average value of $T_{1/2}$ was questionable, the data were correlated with those obtained from the direct-inking oscillograph. A typical comparison of the data obtained from each of the two types of recorders is shown in figure 8. It is seen that while the agreement between the two instruments is generally good, a lack of repeatability in the damping phenomena would introduce random discrepancies in the computed value of $(C_{m_q} + C_{m_{\dot{\alpha}}})$, especially in regions of rapidly changing stability. In view of the poor repeatability of the damping envelopes, the absolute values of $(C_{m_q} + C_{m_{\dot{\alpha}}})$

may be questionable, but at the same time, the use of an average value of the time to damp should permit reasonably accurate performance comparisons to be made between the various model configurations. It should also be noted that these discrepancies in $T_{1/2}$ caused no change in the character of the results.

The derived value of $C_{m\alpha}$, primarily dependent on the accuracy of measurement of model frequency, is considered to be within ± 0.002 . Excellent repeatability of the static stability data was shown for all the models throughout the test Mach number range. However, it should be noted that the value of $C_{m\alpha}$ as used herein is effectively an integrated average value measured between the oscillatory limits of the model ($\approx 14^\circ$) and is correct or incorrect to the extent that the actual slope of the moment curve in this angle-of-attack range is or is not linear.

The results of wind-off model oscillations indicated that the magnitude of the strain-gage-beam resistance greatly exceeded that of the bearing frictional forces. Bearing friction, tending to improve damping characteristics, should vary with tunnel conditions; whereas the strain-gage-beam resistance, affecting both damping and static pitching moment through its own structural damping, should remain essentially constant. As a first approximation to the magnitude of the effect of this combination of forces on model damping, the rotational damping coefficient was calculated for several tunnel conditions and model configurations by using the time to damp determined from wind-off conditions. It was concluded from this approximate analysis that the effect of frictional forces on damping was negligible and that the strain-gage-beam restoring moment affected the magnitude of $(C_{mq} + C_{m\dot{\alpha}})$ only minutely, about 5 percent in the most extreme case.

RESULTS AND DISCUSSION

The results of this investigation are presented as the variation of the dynamic stability coefficient $C_{mq} + C_{m\dot{\alpha}}$ and the static longitudinal stability parameter $C_{m\alpha}$ with Mach number for each primary configuration and for each modification thereto. In addition schlieren photographs are shown at selected test Mach numbers for both the primary and modified model configurations.

Mark-6. - The dynamic and static stability characteristics of the Mark-6 and the effects of modifications thereto are shown in figures 9 to 15. The variations of $C_{mq} + C_{m\dot{\alpha}}$ and $C_{m\alpha}$ with Mach number, while

showing effects of modifications to the primary configuration, did not appreciably change in character.

A sudden trend toward dynamic instability occurs at a Mach number of about 0.84 with the configuration becoming unstable at a Mach number of about 0.86. Above a Mach number of about 0.92 dynamic stability was restored and increased rapidly to a Mach number of about 0.99 where a second destabilizing break occurred. There is a leveling-off tendency above a Mach number of 1.0 to a value similar in magnitude to that shown for the low Mach numbers.

The variation of the static stability parameter, $C_{m\alpha}$, is generally the inverse of that shown for dynamic stability. There is a rapid increase in static stability above a Mach number of about 0.85, a sudden decrease above a Mach number of 0.90, with a small region of low amplitude ($\pm 1.5^\circ$) static instability occurring near a Mach number of 0.97 followed by a general leveling-off tendency at Mach numbers greater than 0.97. Static tests of this configuration to a Mach number of 0.95 have indicated a nonlinear pitching-moment curve with a region of static instability appearing near an angle of attack of zero. This region of static instability first appears near a Mach number of 0.92 and increases in magnitude as the Mach number increases.

The effects of spoiler bands together with the growth and movement of the body shock waves on local flow patterns can be seen from the typical schlieren photographs of figure 9(c). The complex nature of the flow over these bodies makes the derivation of an intelligent concept of flow analysis that would concur with variations in stability extremely difficult.

At a Mach number of 0.8 the supersonic flow field over the model nose and the accompanying discontinuities from the spoiler bands are shown to have terminated in a strong normal shock with a high degree of turbulence or separated flow behind the spoilers and shock patterns. Apparently, initial separation occurs through the foot of a smaller shock forming just ahead of the forward spoiler band. As the Mach number is increased the terminal shock moves downstream with increasingly adverse effects on the flow over the afterbody. These adverse effects are associated with the loss of dynamic stability in the Mach number region 0.84 to 0.92.

As shown in later photographs, this shock reaches the fin leading edge at a Mach number of about 0.94. The flow from the spoiler bands is shown to be increasingly disturbed up to a Mach number of about 0.93, while at higher Mach numbers this flow apparently begins to reattach to the body surface. The rapid variations in dynamic stability shown in the Mach number range from 0.94 to 0.99 are associated with the passage of the normal shock across the fins. The movement of this shock to the

DECLASSIFIED

trailing edge of the model is reflected by the general leveling-off of stability at Mach numbers greater than 1.0.

Previous investigations of these special shapes have indicated that Reynolds number has an effect on the dynamic stability characteristics of these bodies. In an attempt to increase the effective Reynolds number, all configurations with the one exception shown in figure 9 have been tested with artificial roughness on the nose and tail sections as shown in figure 1. The effects of this artificial roughness were evaluated by conducting tests with and without the roughness present and the results are shown in figure 9. No discernible effect on either dynamic or static stability was noted, indicating that transition occurred on the nose at a point less than 0.704 to 0.900 inch from the nose flat. As previously stated, severe pitting of the models by stream suspended particles might tend to mask any effects of this artificial roughness. These results are not construed to indicate that the configuration was insensitive to Reynolds number but that the flow was controlled primarily by the body contour and spoiler bands which gave the described stability characteristics.

In a further attempt to evaluate the effects of Reynolds number on the Mark-6, models of two different sizes were tested. This induced a change in Reynolds number from about 2.15×10^6 to 2.5×10^6 . While the effects of changing Reynolds number are masked somewhat by scatter in the data and the fact that comparable data are available only in a region of rapid variation of dynamic stability with Mach number, reducing the Reynolds number appears to lower the Mach numbers at which sudden changes occur by approximately 0.015, as shown in figure 10. The static stability characteristics of the Mark-6 indicated no appreciable variation with changing Reynolds number.

Presented in reference 4 are comparison data for wind-tunnel and full-scale models of the Mark-6. These data, while not conclusive, indicate that care should be exercised in the extrapolation of data obtained at the relatively low Reynolds numbers of wind-tunnel tests to full-scale Reynolds numbers. Results presently available do not clearly define the effects of Reynolds number on models of this type.

An investigation was made to determine the effects of center-of-gravity movement on the stability characteristics of the Mark-6. The results are presented in figure 11. As the center of gravity was moved rearward 9.2 inches (full scale) there was a definite trend toward a lower level of dynamic stability. The Mach number region of dynamic instability was increased by approximately 0.02. This increase in the Mach number range where dynamic instability exists appears to result from a displacement of the curve rather than a change in character. The changes in static stability resulting from movement of the center of gravity were as expected, although calculations could not be made for a disturbed flow of this nature.

To evaluate the effects of suspension lugs mounted in the pitch plane on the stability characteristics of the Mark-6 tests were conducted with a single lug at model station 2 and a double lug arrangement at model stations 1 and 3 (see fig. 3). The results of these tests are presented in figure 12. While certain differences in magnitude of the stability parameters exist for the various lug positions, no consistent trends can be detected. The schlieren photographs of figure 12(c) show the effects of the lugs and their various positions on the local flow patterns. From these photographs, the greatest disturbance of the local boundary layer was apparently caused by the most forward lug (position 1, fig. 3), since the lugs in positions 2 and 3 were in a highly turbulent or separated flow region induced by the spoiler bands. However, the disturbances from these lugs would necessarily be highly localized and would probably affect the stability characteristics of the model only through small changes in the angle of trim. Trim changes of the order of 0.8° were observed for the model with lugs at positions 1 and 3.

Tests were conducted to determine the effects of using a 4° - 20° fin (see fig. 2(d)) in place of the 5° - 25° fin. The results, presented in figure 13, indicated that while a small decrease in the Mach number region of dynamic instability was achieved by this change, a reduction in static stability occurred through the Mach number range above 0.85 with static instability occurring in the Mach number range from 0.97 to 1.02. In the Mach number region near 1.0 the model attempted to trim at an angle of attack exceeding the limits of the test apparatus ($\pm 4^\circ$).

Results of an investigation to determine the effects on stability of the addition of two diametrically opposed, fin-mounted, fan ducts (see fig. 2(c)) are presented in figure 14. These results indicate no appreciable change in either dynamic or static stability due to the addition of the fan ducts. The slight tendency toward higher dynamic stability for the ducted configuration is considered to be within the scatter of the data since the comparison is made in a region of rapid variation with Mach number.

An examination of the schlieren photographs for the ducted configuration would indicate a slight increase in stability due to the stronger shock induced by the ducts. As was the case for the previously discussed alterations to the Mark-6, no large differences were noted in the flow characteristics indicating that no large changes in stability should be expected. The decrease in effective fin area accompanying the installation of the ducts probably reduced any benefit thus obtained.

In figure 15 are shown the results of the addition of fan ducts as well as a change in Reynolds number. When compared with the results shown in figure 10(a) it can be seen that the changes evident in this figure are predominantly caused by Reynolds number. The effect of

DECLASSIFIED

increasing Reynolds number is to shift the region of rapid changes in dynamic stability to higher Mach numbers. It is noted that the difference between the two curves is increased up to a Mach number of about 0.98 and is reduced above this point. It should also be noted that changing Reynolds number does not affect the character of the curves indicating that the effects of Reynolds number are of a secondary nature. While the effects of the ducts are masked by the larger Reynolds number effects it is indicated that the presence of the ducts causes a slight increase in the level of dynamic stability.

Mark-4.-- The results of an investigation to determine the dynamic and static stability characteristics of the Mark-4 configuration are presented in figure 16. This configuration is identical to the Mark-6 in body and fin contour but does not utilize spoiler bands. The effects of these spoiler bands are shown by the comparison of the Mark-4 and Mark-6 configurations.

Removal of the spoiler bands results in an increase in dynamic stability at low Mach numbers and a reduction at the higher Mach numbers. The range in which dynamic instability exists occurs at higher Mach numbers. The static stability of the Mark-4 appears to be generally lower than that for the Mark-6 at Mach numbers below about 0.95, above which the reverse is true.

An examination of high-speed schlieren motion pictures indicates that at the higher Mach numbers the spoiler bands of the Mark-6 tend to stabilize the shock patterns while on the Mark-4 a large fore and aft shift of the strong normal shock is seen to occur as the model oscillates. The tendency previously noted of the separated flow over the rear portion of the Mark-6 to reattach at the higher Mach numbers is apparently counteracted by this fore and aft movement of the shock pattern on the Mark-4.

TX-4.-- Presented in figure 17 are the results of an investigation of the TX-4 configuration. These results indicated no unstable characteristics, either dynamic or static, for this configuration throughout the Mach number range of these tests. The magnitude of the dynamic stability of the TX-4 compares favorably with that of the Mark-6 while the level of static stability is generally lower. The schlieren photographs indicated that for this configuration there was a sharp reduction in the boundary-layer thickness on the nose and separated flow regions.

TX-13.-- Tests were conducted to determine the dynamic and static stability characteristics of two TX-13 models. These configurations were the TX-13B' and the TX-13C. The TX-13B' was tested with three different center-of-gravity locations. Figures 18 and 19 present the results of this investigation.

DECLASSIFIED

In all cases the TX-13B' exhibited a region of static instability in the Mach number range from about 0.95 to 0.99. Changes in the center-of-gravity position of 11 inches (full scale) resulted in no discernible change in this region of static instability.

There appears to be no definite trend in dynamic stability resulting from changes in center of gravity although it should be noted that tests of the configuration with the rearmost center-of-gravity position were conducted at a higher Reynolds number. As previously indicated, Reynolds number appears to have little effect on static stability.

Removal of the spoiler bands and a modification to the nose shape (TX-13C) eliminated the region of static instability, but this change was accompanied by a general decrease in dynamic stability at the higher Mach numbers with a small region of neutral stability (amplitude $\approx \pm 2.5^\circ$) being noted near a Mach number of 0.92. At the lower Mach numbers an increase in dynamic stability accompanied the removal of the spoiler bands as was the case with the previously discussed Mark-4.

An examination of the schlieren photographs of the TX-13B' and the TX-13C (fig. 19(c)) indicate that near a Mach number of 0.92 the TX-13B' exhibits a large region of highly turbulent or separated flow in contrast to the TX-13C. A more rapid rearward movement of the main body shock with increases in Mach number is noted for the TX-13C.

Mark-5.— The Mark-5 configuration exhibited no unstable characteristics, either dynamic or static, throughout the Mach number range of the investigation as shown in figure 20. The level of dynamic stability was generally higher than for the other configurations tested but this model exhibited rapid variations with Mach number in the range of Mach numbers from about 0.85 to 1.0. The static stability in the low Mach number regions was somewhat higher than for the other configurations tested but was of the same order of magnitude above a Mach number of 1.0.

The Mark-5 tended to trim at an angle of attack of about 2° between the Mach numbers of 0.99 and 1.03. This tendency cannot be associated with the suspension lug used since the lug was mounted on the body at 90° from the pitch plane.

The schlieren photographs indicate that the flow over the Mark-5 configuration is in general improved over the bodies previously considered. Since the characteristics of these configurations are influenced primarily by this flow it is apparent that bodies of higher fineness ratio should lead to more desirable characteristics.

DECLASSIFIED

CONCLUDING REMARKS

From an investigation of the dynamic and static stability characteristics of the Mark-6, Mark-4, TX-4, TX-13, and Mark-5 special weapons in the Mach number range from 0.70 to 1.10, the following observations are made:

Mark-6.- In all cases investigated the Mark-6 displayed a region of dynamic instability in the Mach number range between 0.84 to 0.86 and 0.92 to 0.94, with performance above and below this region being generally satisfactory. A small region of low amplitude static instability was indicated near a Mach number of 0.97.

The addition of artificial roughness to the nose and fins of the Mark-6 showed no discernible effect on either the dynamic or static characteristics.

Tests of the Mark-6 at two different Reynolds numbers indicated that a reduction in Reynolds number would lower the Mach number at which sudden changes in dynamic stability occur by approximately 0.015 but would have little effect on static stability.

A rearward movement of the center of gravity of the Mark-6 resulted in a lower level of dynamic stability with the Mach number region of dynamic instability being increased by about 0.02.

The addition of a single or double lug suspension arrangement to the Mark-6 caused no appreciable change in the stability characteristics. A small change in trim angle (less than 1°) was indicated to result from the double lug arrangement.

The use of 4° - 20° fins on the Mark-6 resulted in a small decrease in the Mach number range of dynamic instability but was accompanied by an increased region of static instability near a Mach number of 1.0.

The addition of two diametrically opposed, fin-mounted, fan ducts to the Mark-6 resulted in no appreciable change in stability although a slight tendency toward higher dynamic stability was noted.

Mark-4.- The Mark-4 configuration exhibited an increase in dynamic stability at low Mach numbers over that of the Mark-6 and a reduction at the higher Mach numbers with the region of dynamic instability occurring at higher Mach numbers. The static stability of the Mark-4 was generally lower than that for the Mark-6 at Mach numbers below 0.95 above which the reverse was true.

DECLASSIFIED

TX-4.- The TX-4 configuration exhibited no unstable characteristics, either dynamic or static, throughout the Mach number range of this investigation. The magnitude of the dynamic stability compared favorably with that of the Mark-6 while the level of static stability was generally lower.

TX-13.- In all cases the TX-13B' exhibited a region of static instability in the Mach number range from about 0.95 to 0.99. A change in center-of-gravity location corresponding to 11 inches full scale resulted in no discernible change in this region of static instability.

The TX-13C exhibited no region of static instability such as that noted for the TX-13B'. The TX-13C indicated a general decrease in dynamic stability at the higher Mach numbers with a small region of neutral stability of $\pm 2.5^\circ$ amplitude being noted near a Mach number of 0.92.

Mark-5.- The Mark-5 configuration exhibited no unstable characteristics, either dynamic or static, throughout the Mach number range investigated. The level of dynamic stability was generally higher than for the other configurations tested but exhibited rapid variations with Mach number in the range of Mach numbers from about 0.85 to 1.0.

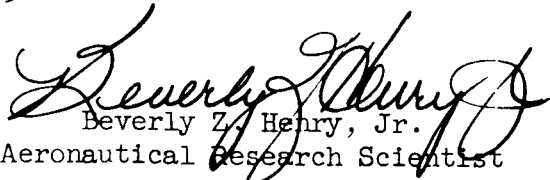
Reynolds number effects.- The results of this and other investigations have indicated that Reynolds number may have an effect on the dynamic performance of configurations of this type. For this investigation the effects of Reynolds number change were to alter the Mach number at which sudden changes in dynamic stability occurred while the character of the dynamic performance remained essentially the same indicating that Reynolds number is probably of a secondary nature. Sufficient information is not presently available to predict the exact nature of these effects and until such time as this information becomes available, care should be exercised in the extrapolation of wind-tunnel results to full-scale conditions.

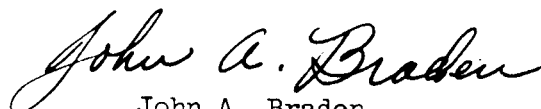
General.- The configurations which exhibited the more desirable performance characteristics were in general those which were less subject to a highly complex or separated flow. Improvements in the

DECLASSIFIED

local flow conditions would therefore be expected to have an advantageous effect on the stability performance of these bodies.

Langley Aeronautical Laboratory,
National Advisory Committee for Aeronautics,
Langley Field, Va., July 3, 1953.


Beverly Z. Henry, Jr.
Aeronautical Research Scientist


John A. Braden
Aeronautical Research Scientist

Approved:


Eugene C. Draley
Chief of Full-Scale Research Division

cg



REF ID: A53609c

NACA RM SL53G09c

REFERENCES

1. Wright, Ray H., and Ritchie, Virgil S.: Characteristics of a Transonic Test Section With Various Slot Shapes in the Langley 8-Foot High-Speed Tunnel. NACA RM L51H10, 1951.
2. Ritchie, Virgil S., and Pearson, Albin O.: Calibration of the Slotted Test Section of the Langley 8-Foot Transonic Tunnel and Preliminary Experimental Investigation of Boundary-Reflected Disturbances. NACA RM L51K14, 1952.
3. Davis, Milton W., and Clark, Edwin T.: Pre-Test Information Transonic Dynamic Stability Wind Tunnel Tests of MK-5, MK-6, and TX-13 Special Weapons. Ref. Sym: 5142 (3), Sandia Corporation, Albuquerque, New Mexico, Sept. 20, 1952.
4. Clark, Edwin T.: Free Flight and Wind Tunnel Damping Characteristics of the Standard MK-6. Ref. Sym: 5141 (313), Sandia Corporation, Albuquerque, New Mexico, Oct. 21, 1952.

TABLE I

(a) MARK 4				I
N ₄₀ ^{6.5}	B ₄₀	G _{39.8}	R ₂₈₀ ^{NF} F ₅₋₂₅	0.0450

(c) TX-4				I
N ₄₀ ^{6.5}	B _{TX-4}	G _{39.8}	R ₂₈₀ ^{NF} F ₁₂	0.0558

(b) MARK 6						I
N ₄₀ ^{6.5}	B ₄₀	G _{39.8}	R ₂₈₀ ^{NF} S _E	F ₅₋₂₅		0.0450
N ₄₀ ^{6.5}				2 F ₅₋₂₅ 2 F ₅₋₂₅ D ¹⁻³		0.0445
N ₄₀ ^{7.5}				F ₅₋₂₅		0.1244
						0.1244
						0.0958
						0.0958
						0.0958
						0.1296

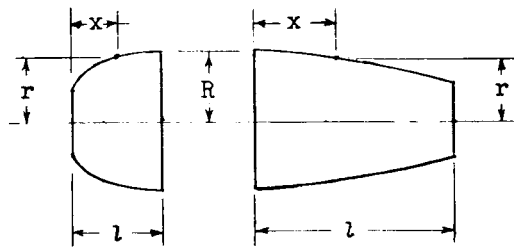
(d) TX-13B ¹						I
N ₄₀ ^{6.5}	E ₁₇	B ₄₀	G _{60.9}	R ₂₈₀ ^{NF} F ₅₋₂₅	S _{367.99}	0.0524
N ₄₀ ^{6.5}						0.0474
N ₄₀ ^{7.5}						0.1175

(e) TX-13C				I
N ₅₀ ^{7.5}	E ₁₇	B ₄₀	G _{62.0} R ₂₈₀ ^{NF} F ₅₋₂₅	0.1120

(f) MARK 5				I
N ₅₄ ^{6.5}	B ₅₄	G _{40.4}	R ₂₈₀ ^{NF} F ₁₆₋₀ t	0.0878

NACA

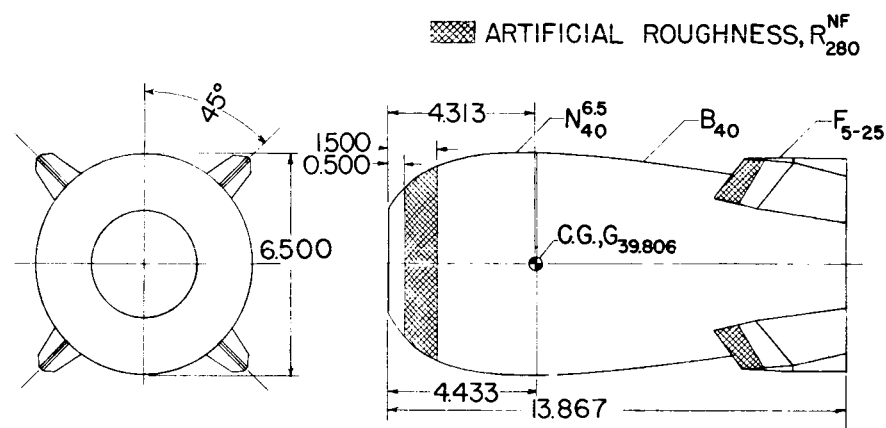
TABLE II



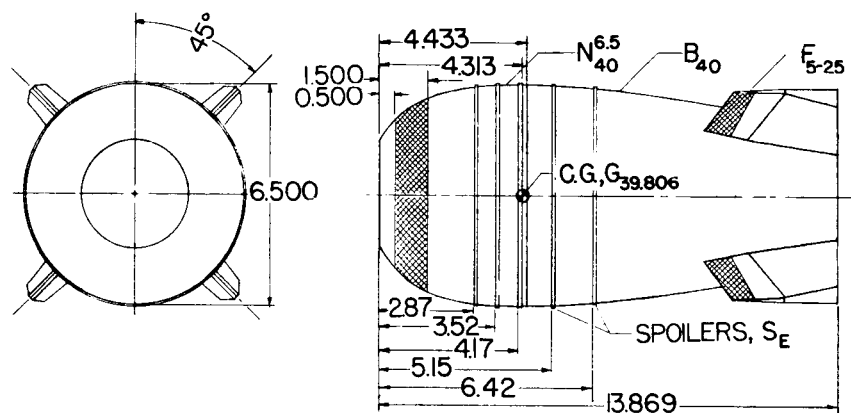
NOSE COORDINATES					
N_{40}		N_{50}		N_{54}	
x/l	r/R	x/l	r/R	x/l	r/R
0	0.483	0	0.450	0	0.617
.049	.532	.049	.529	.067	.679
.098	.663	.098	.595	.133	.731
.147	.725	.147	.651	.200	.777
.196	.778	.195	.700	.267	.817
.244	.821	.244	.742	.333	.851
.293	.857	.293	.781	.400	.882
.342	.886	.342	.814	.467	.906
.391	.910	.391	.844	.533	.930
.449	.947	.439	.895	.600	.949
.587	.971	.587	.934	.667	.965
.684	.986	.684	.963	.733	.978
.782	.994	.782	.984	.800	.988
.880	.998	.880	.996	.867	.994
1.000	1.000	.977	1.000	.933	.999
		1.000	1.000	1.000	1.000

AFTERBODY COORDINATES					
B_{40}		B_{TX-4}		B_{54}	
x/l	r/R	x/l	r/R	x/l	r/R
0.035	0.998	0	1.000	0	1.000
.031	.994	.265	1.000	.020	.999
.127	.986	.373	.960	.041	.994
.173	.977	1.000	.750	.051	.991
.219	.967			.061	.986
.265	.956			.071	.983
.357	.926			1.000	.542
.449	.891				
.518	.862				
.598	.824				
.632	.806				
.656	.792				
1.000	.550				

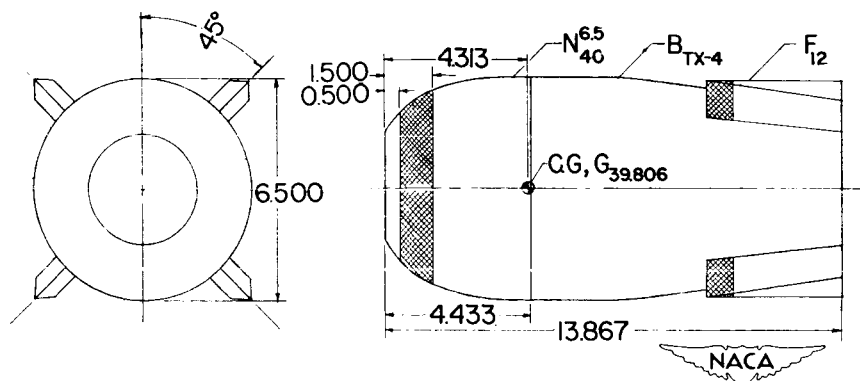
DECLASSIFIED



(a) MARK 4



(b) MARK 6

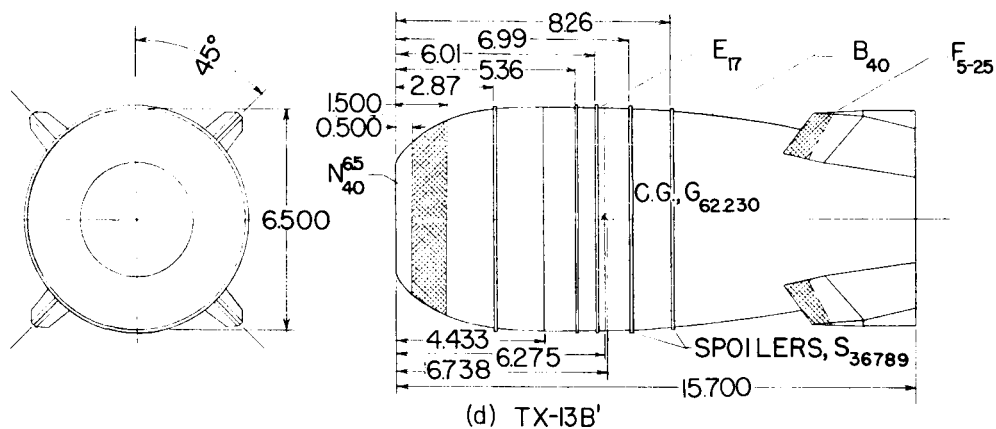


TX-4

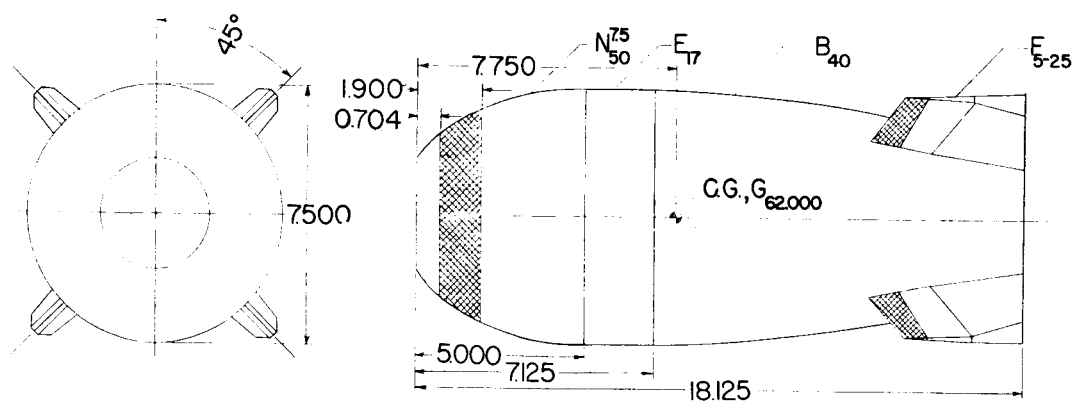
Figure 1.- Details of the model configurations tested. All dimensions are in inches.

DECLASSIFIED

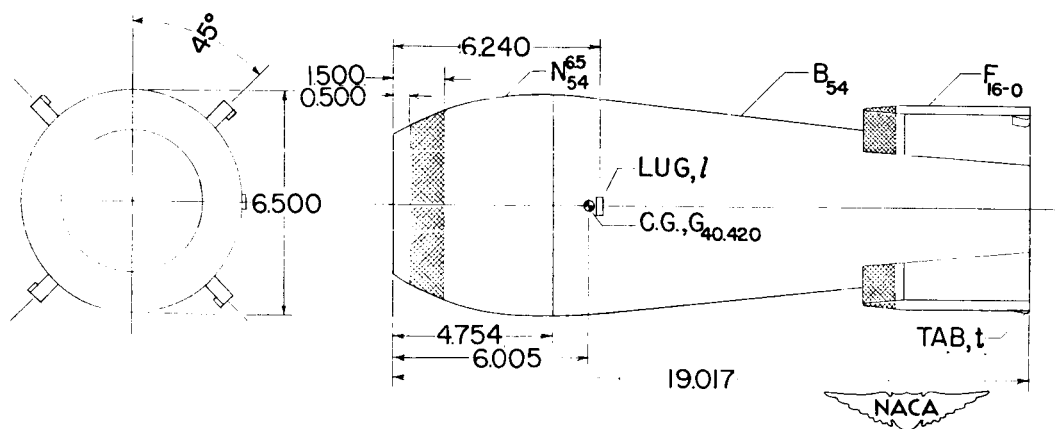
ARTIFICIAL ROUGHNESS, R_{280}^{NF}



(d) TX-13B'



(e) TX-13C



(f) MARK-5

Figure 1.- Concluded.

DECLASSIFIED

ARTIFICIAL ROUGHNESS, R_{280}^F

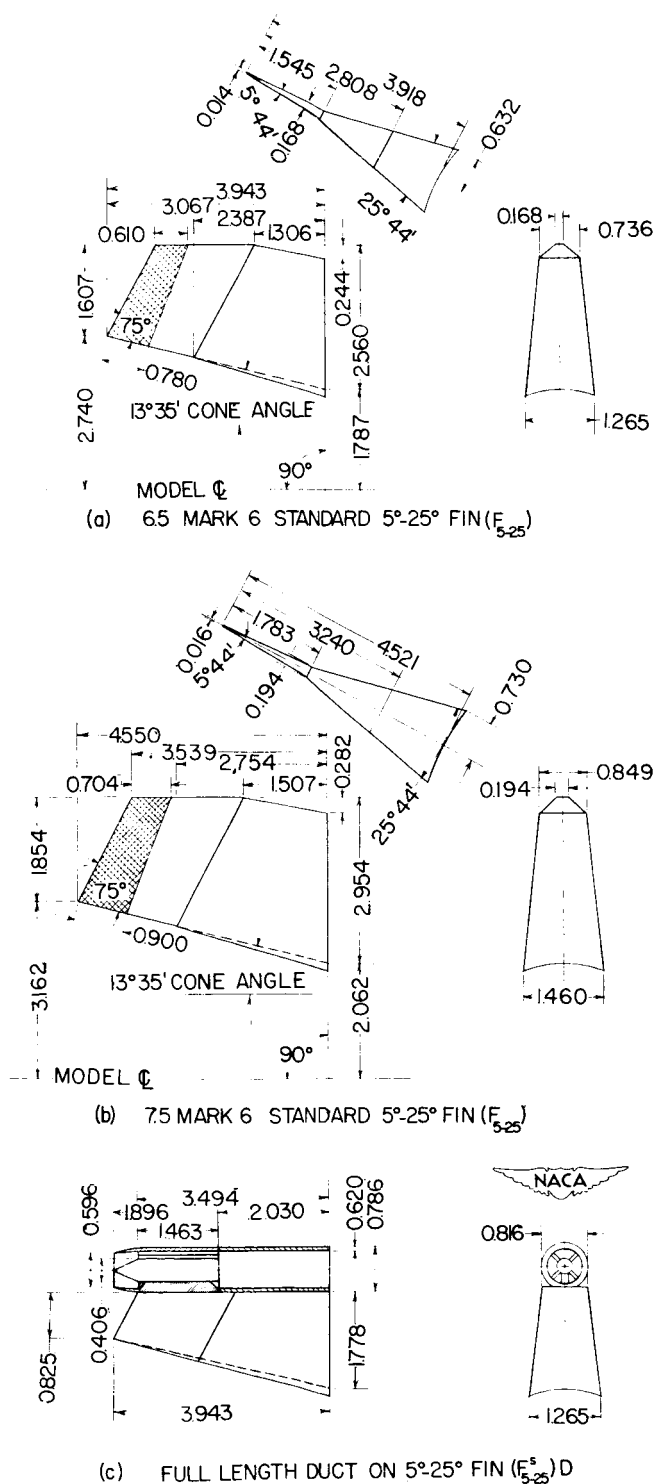


Figure 2.- Details of the stabilizing fins. All dimensions are in inches.

REPRODUCED

ARTIFICIAL ROUGHNESS, R_{280}^F

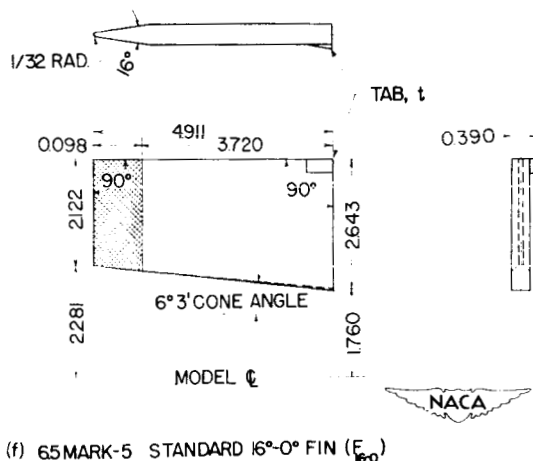
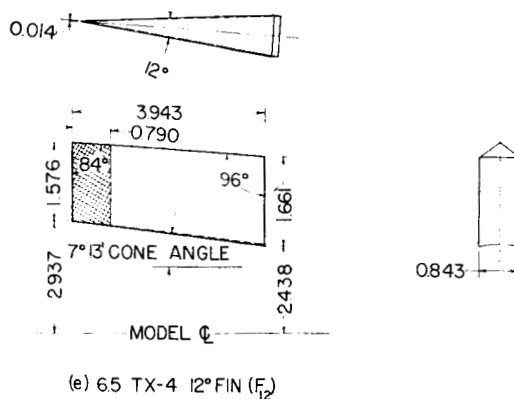
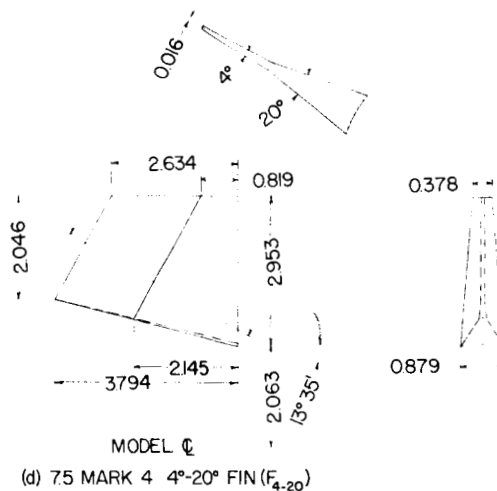


Figure 2.- Concluded.

SECRET

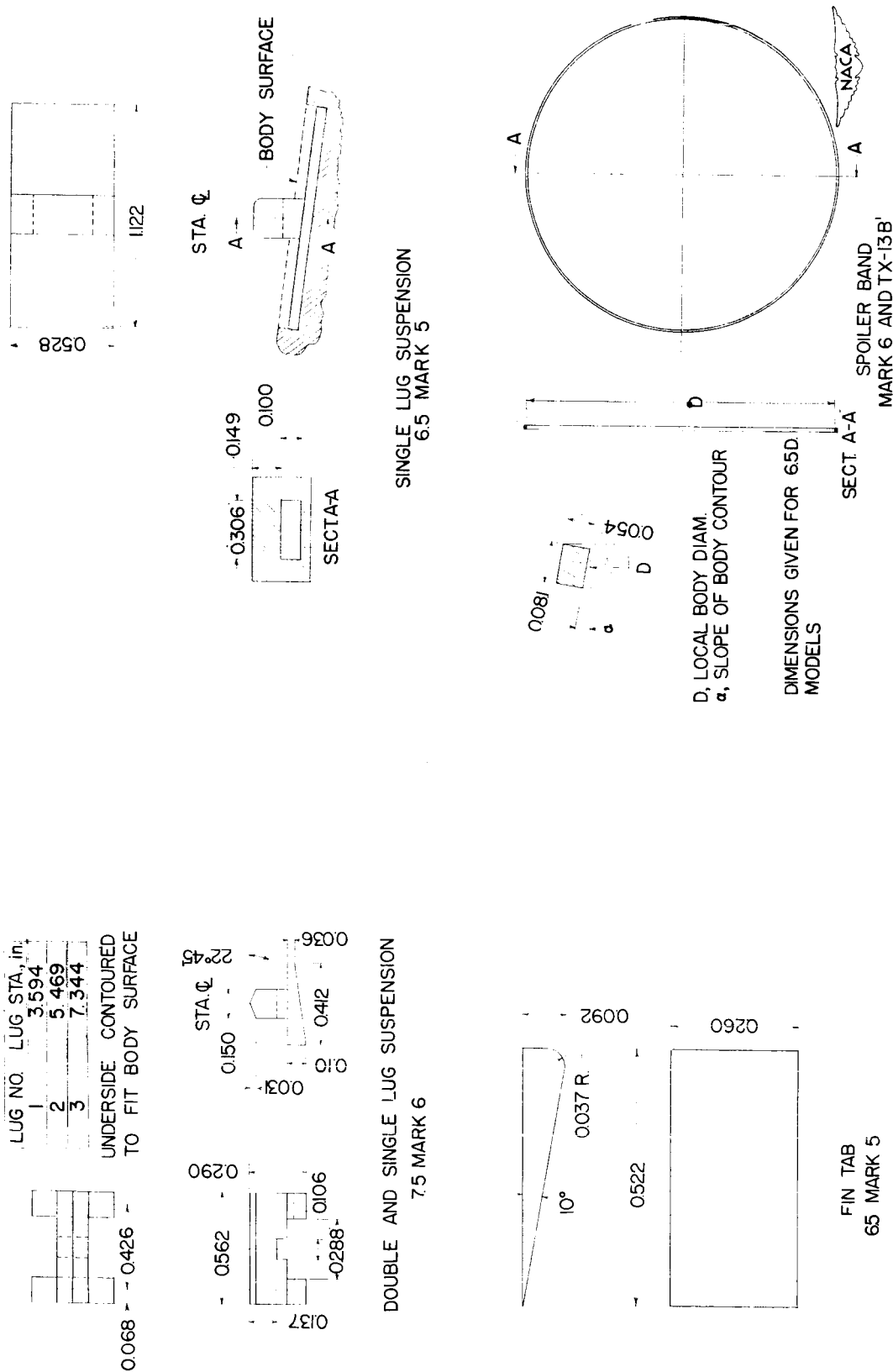


Figure 3.- Details of accessory parts used with the models. All dimensions are in inches.

DECLASSIFIED

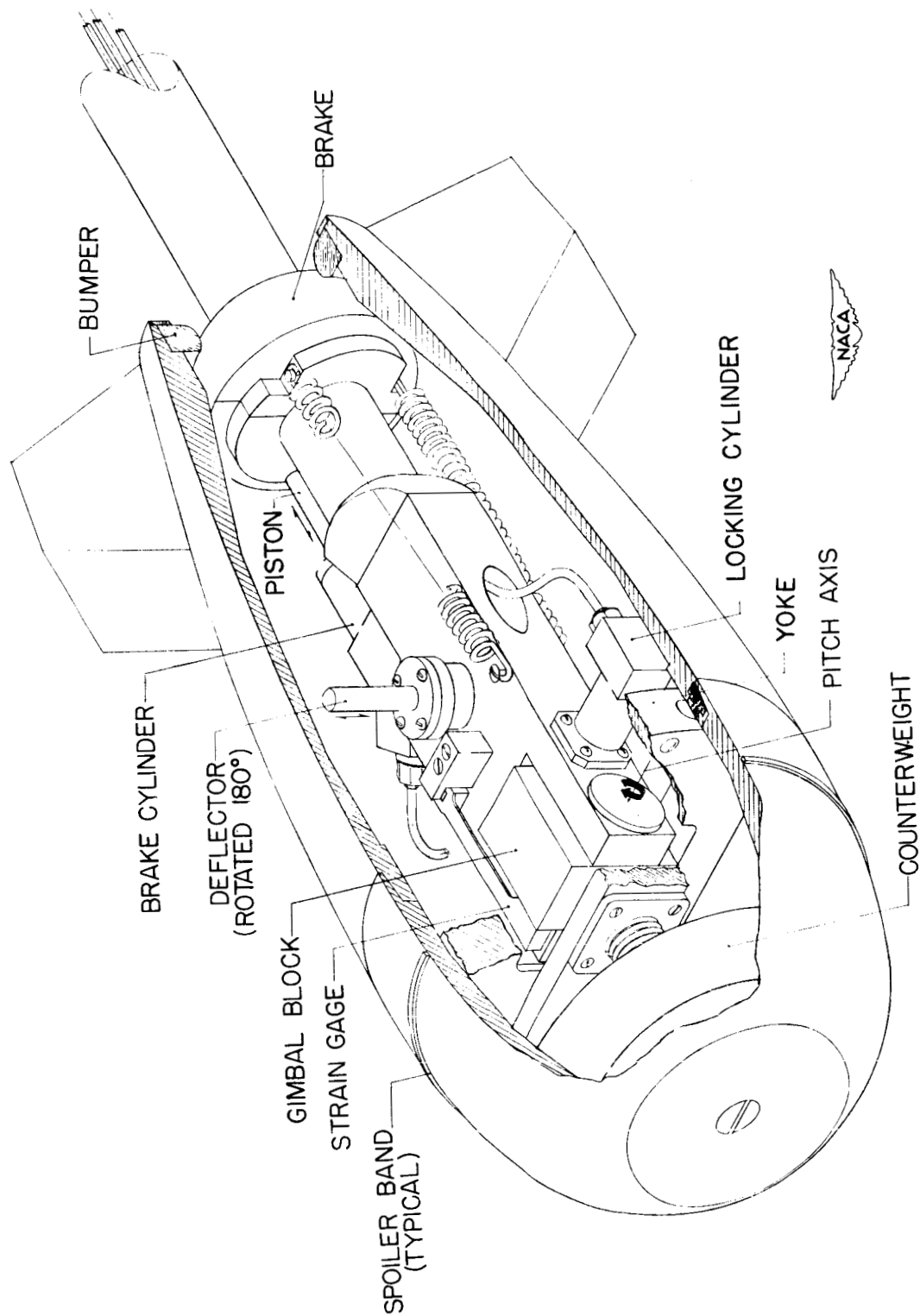


Figure 4.- Details of a typical model installation on the dynamic testing apparatus.

DECLASSIFIED

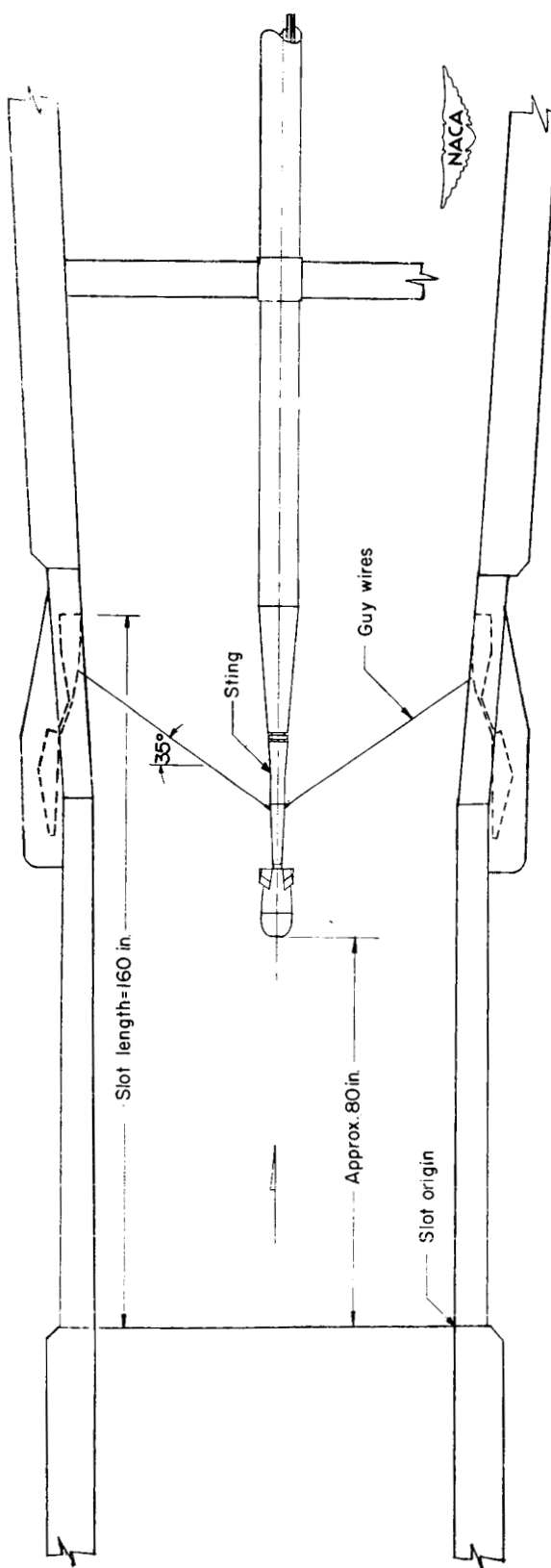
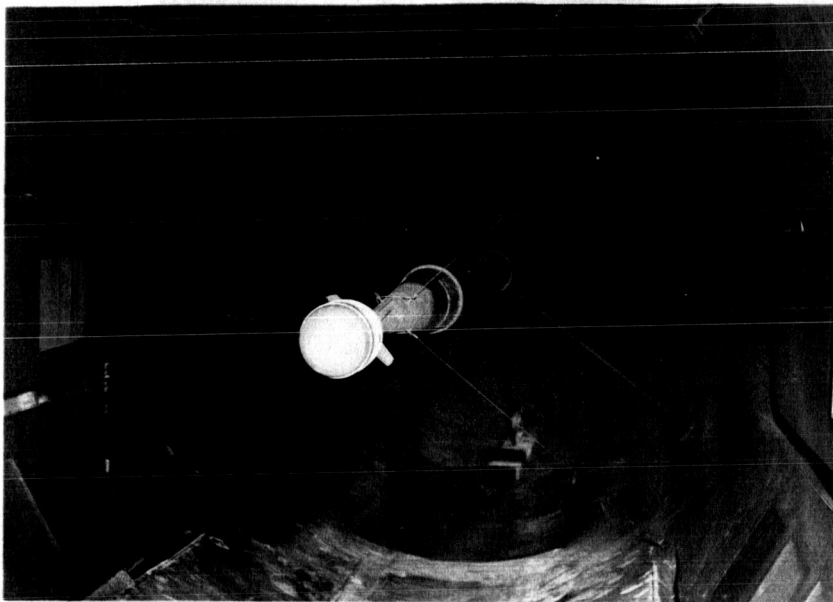
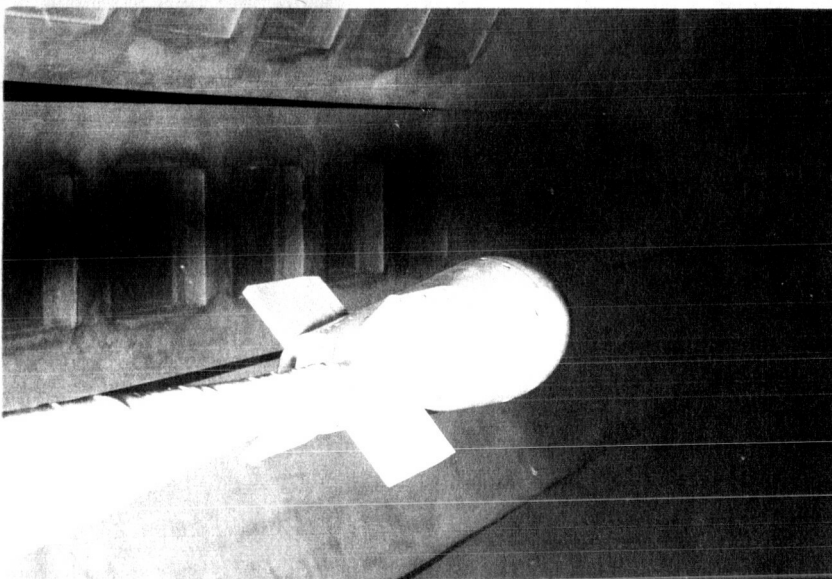


Figure 5.- General arrangement of a typical model installation in the 8-foot transonic tunnel. All dimensions are in inches.

DECLASSIFIED



RDP No. 246



RDP No. 244

Figure 6.- Photographic views of models mounted in the test section.

DECLASSIFIED

SECRET

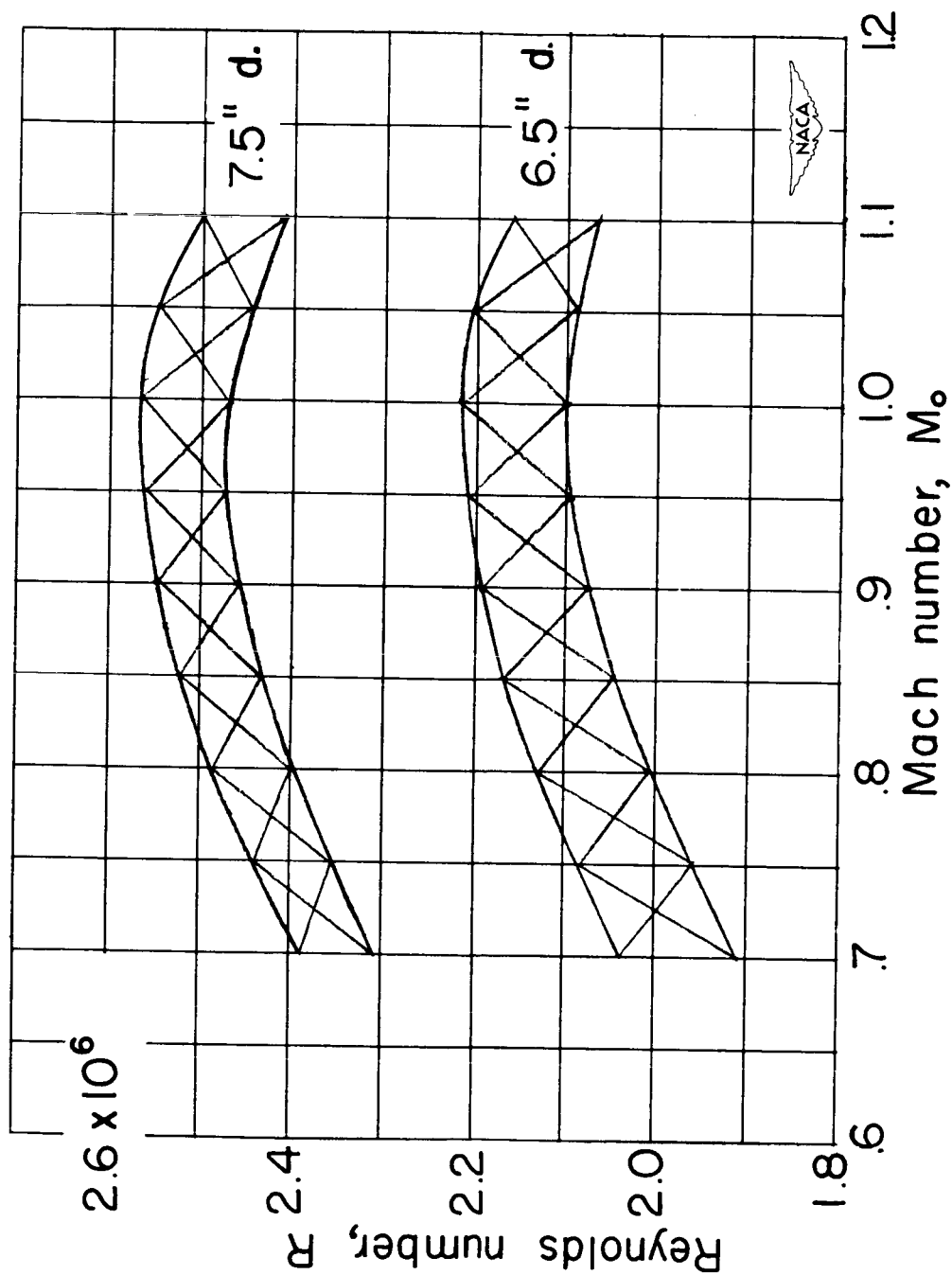


Figure 7.- Variation of Reynolds number, based on d , in the 8-foot transonic tunnel.

REF ID: A53609

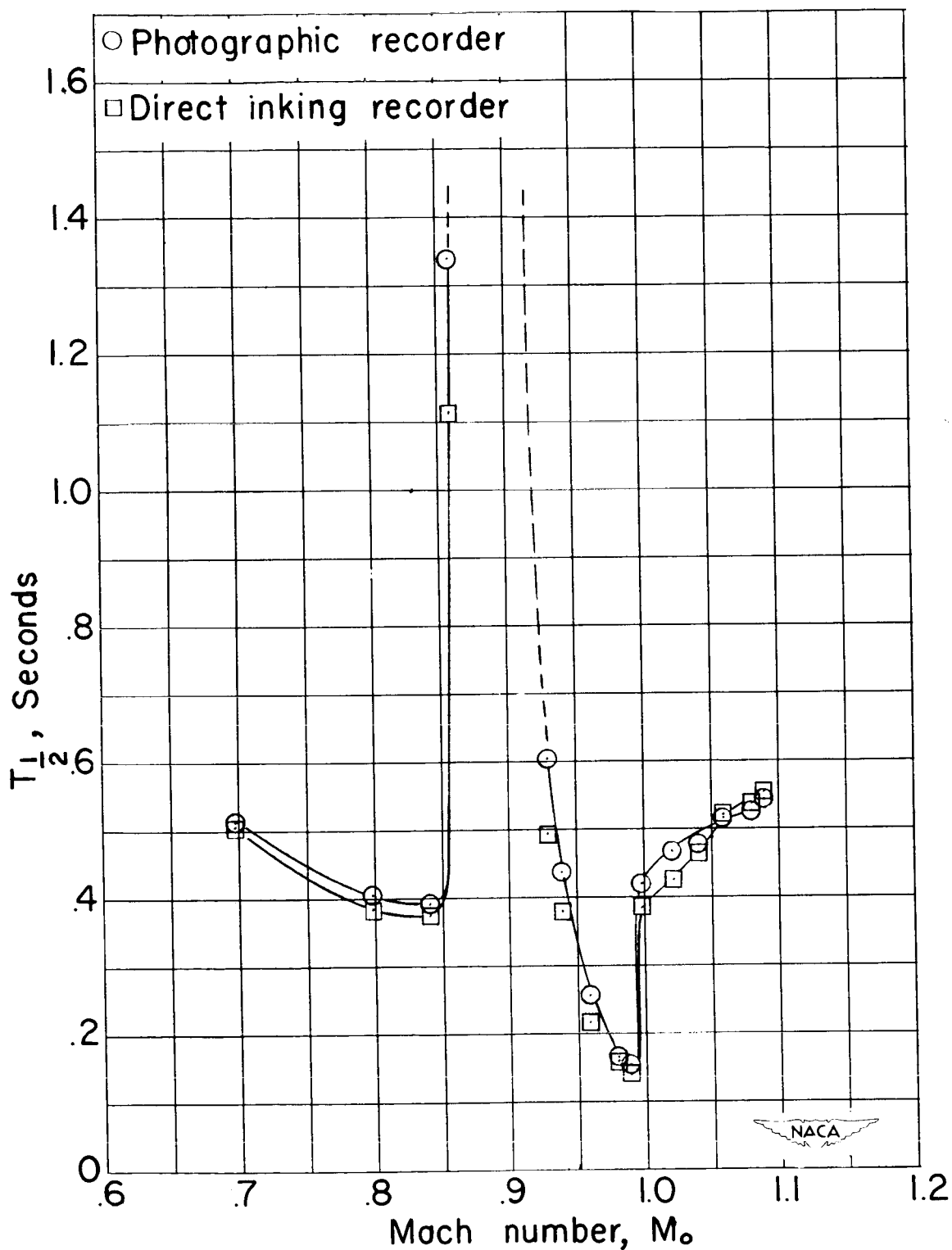
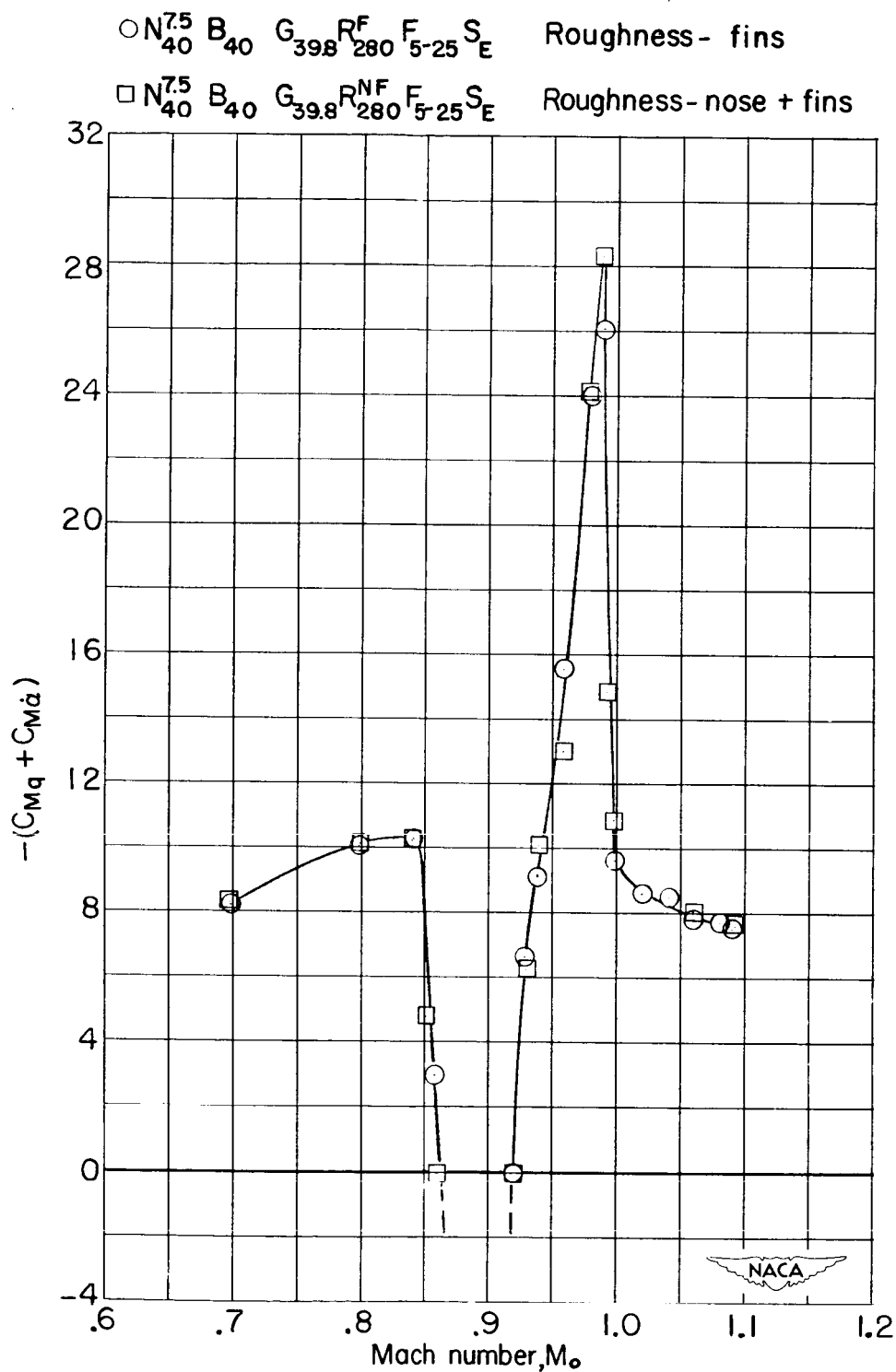


Figure 8.- Comparison of results obtained from the two instruments used in the investigation.

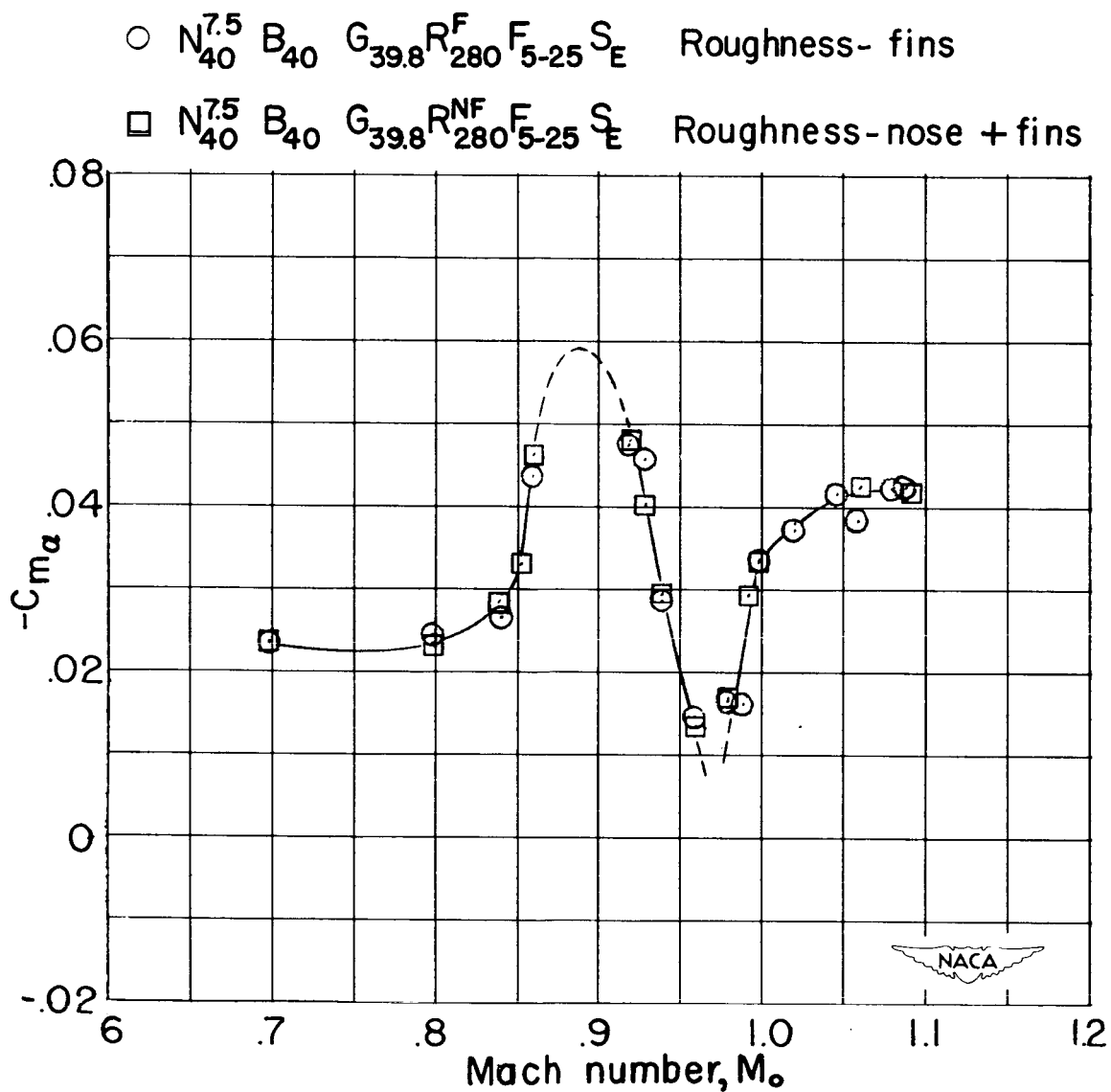
DECLASSIFIED



(a) Dynamic stability.

Figure 9.- The dynamic and static stability characteristics of the Mark-6 configuration and the effects of the addition of artificial roughness.

DECLASSIFIED

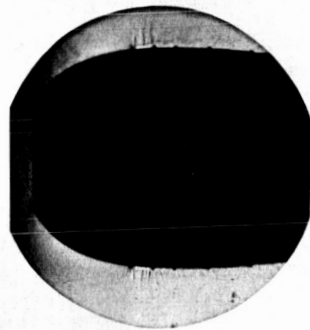


(b) Static stability.

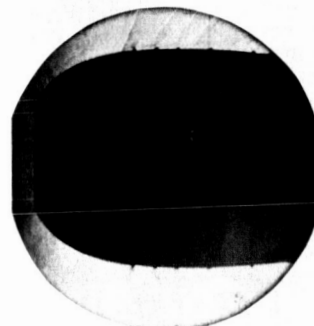
Figure 9.- Continued.

DECLASSIFIED

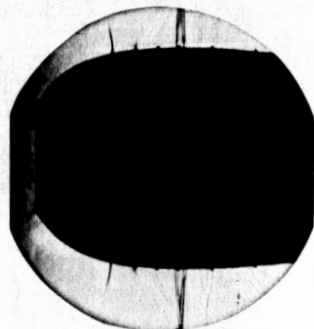
Mark 6



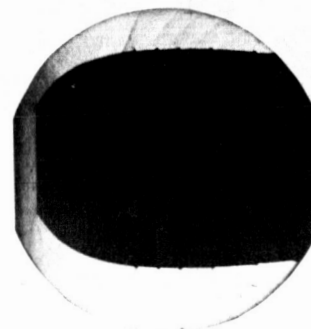
$M_o=0.70$



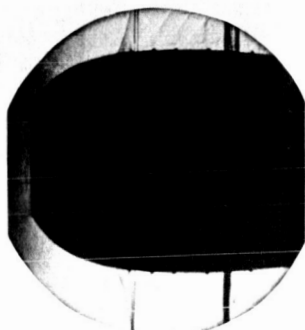
$M_o=0.92$



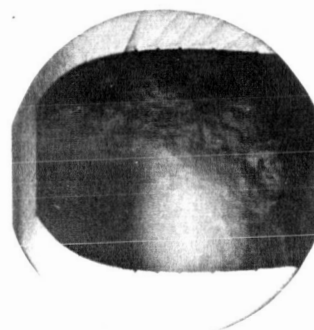
$M_o=0.80$



$M_o=1.00$



$M_o=0.86$



$M_o=1.09$

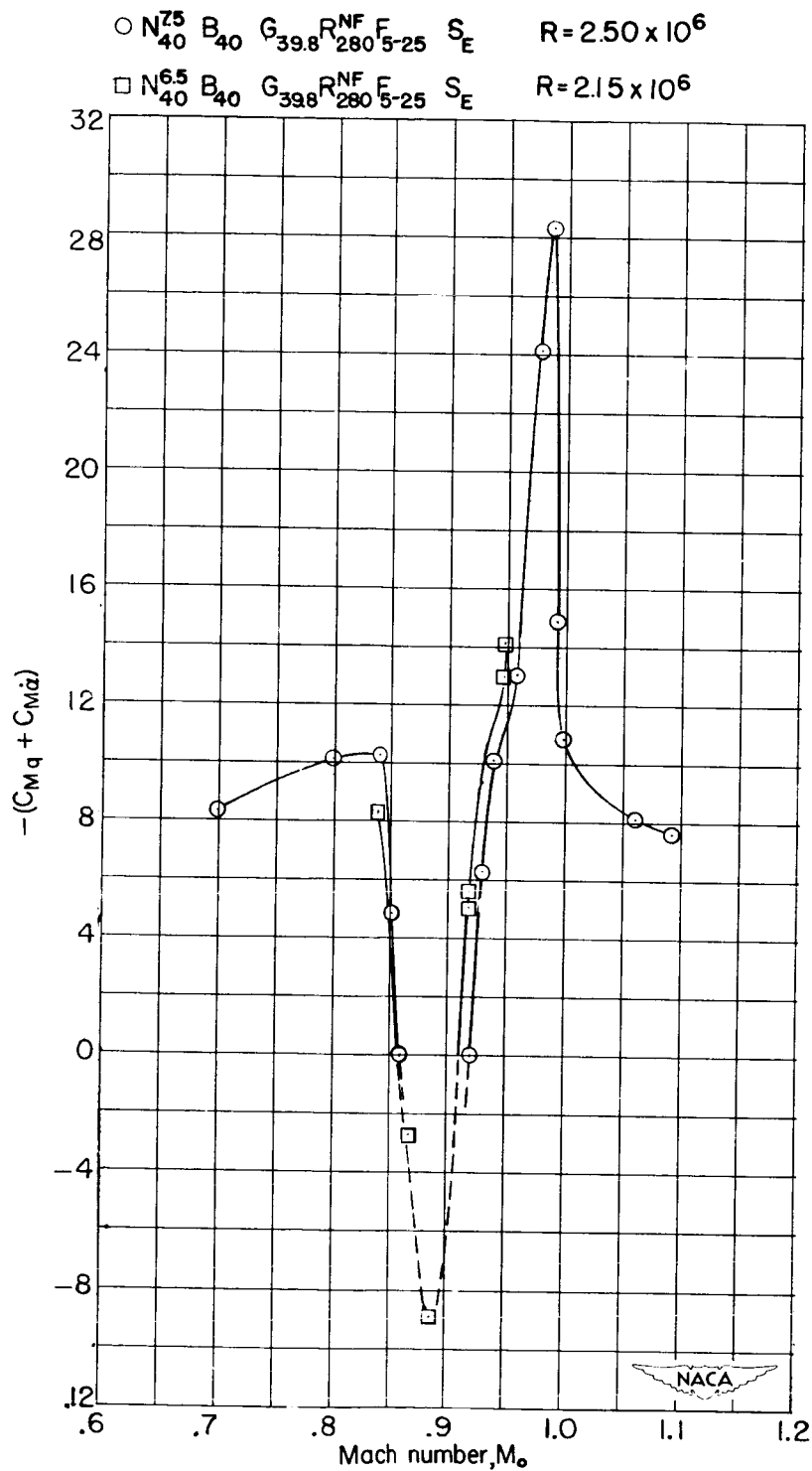
(c) Schlieren photographs of model with roughness.



Figure 9.- Concluded.

RDP No. 250

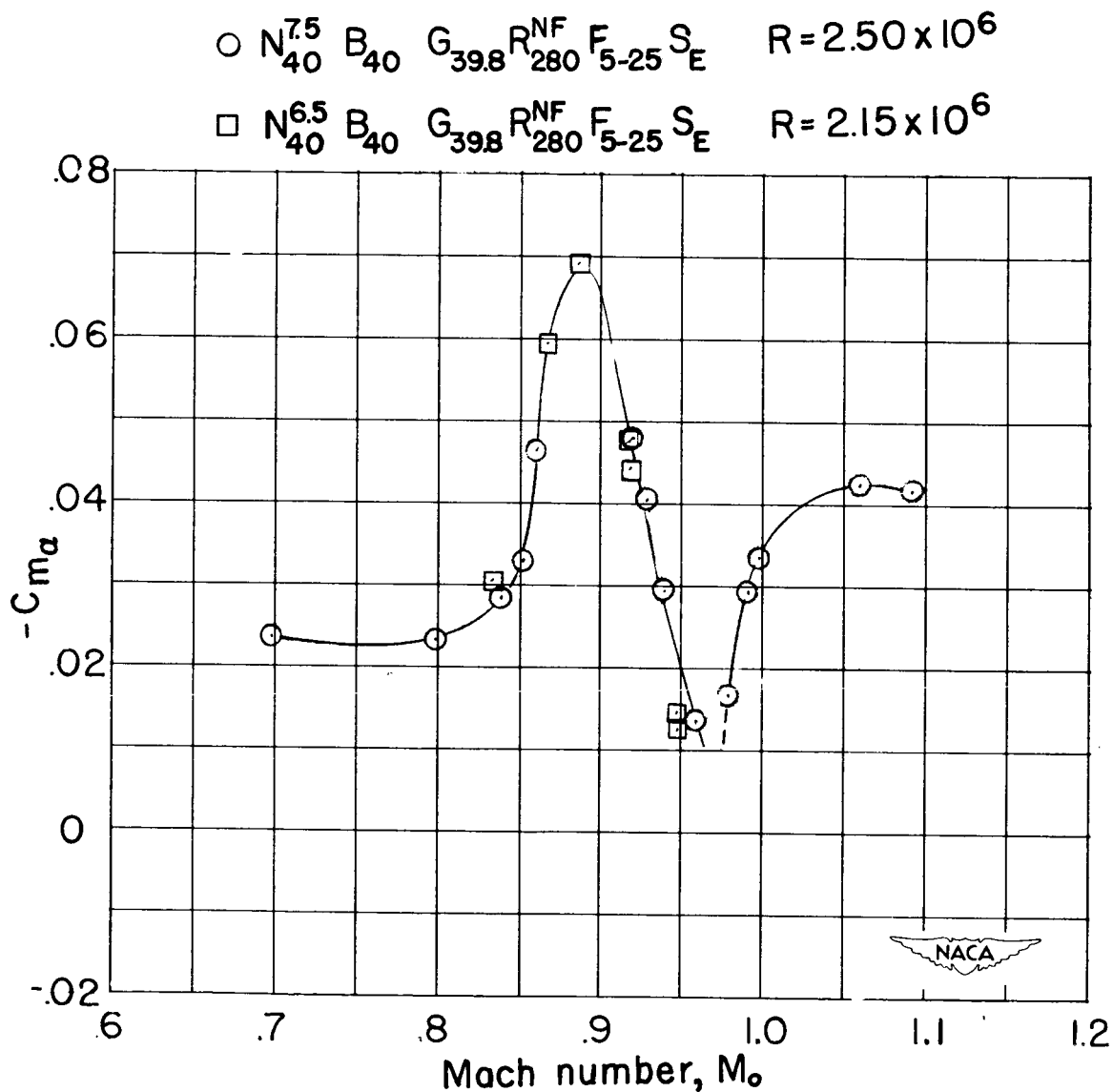
DECLASSIFIED



(a) Dynamic stability.

Figure 10.- The effects of Reynolds number on the stability characteristics of the Mark-6.

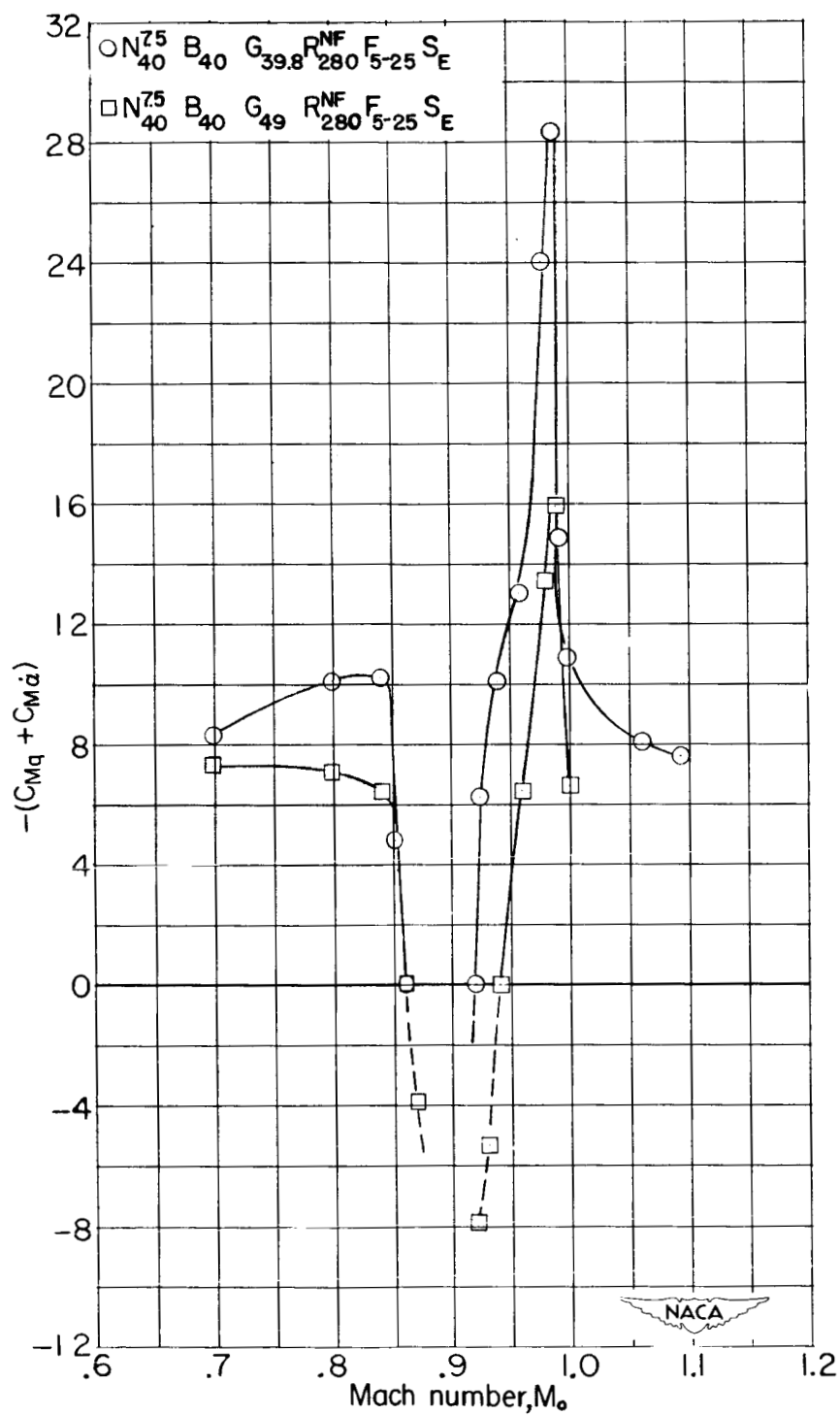
DECLASSIFIED



(b) Static stability.

Figure 10.- Concluded.

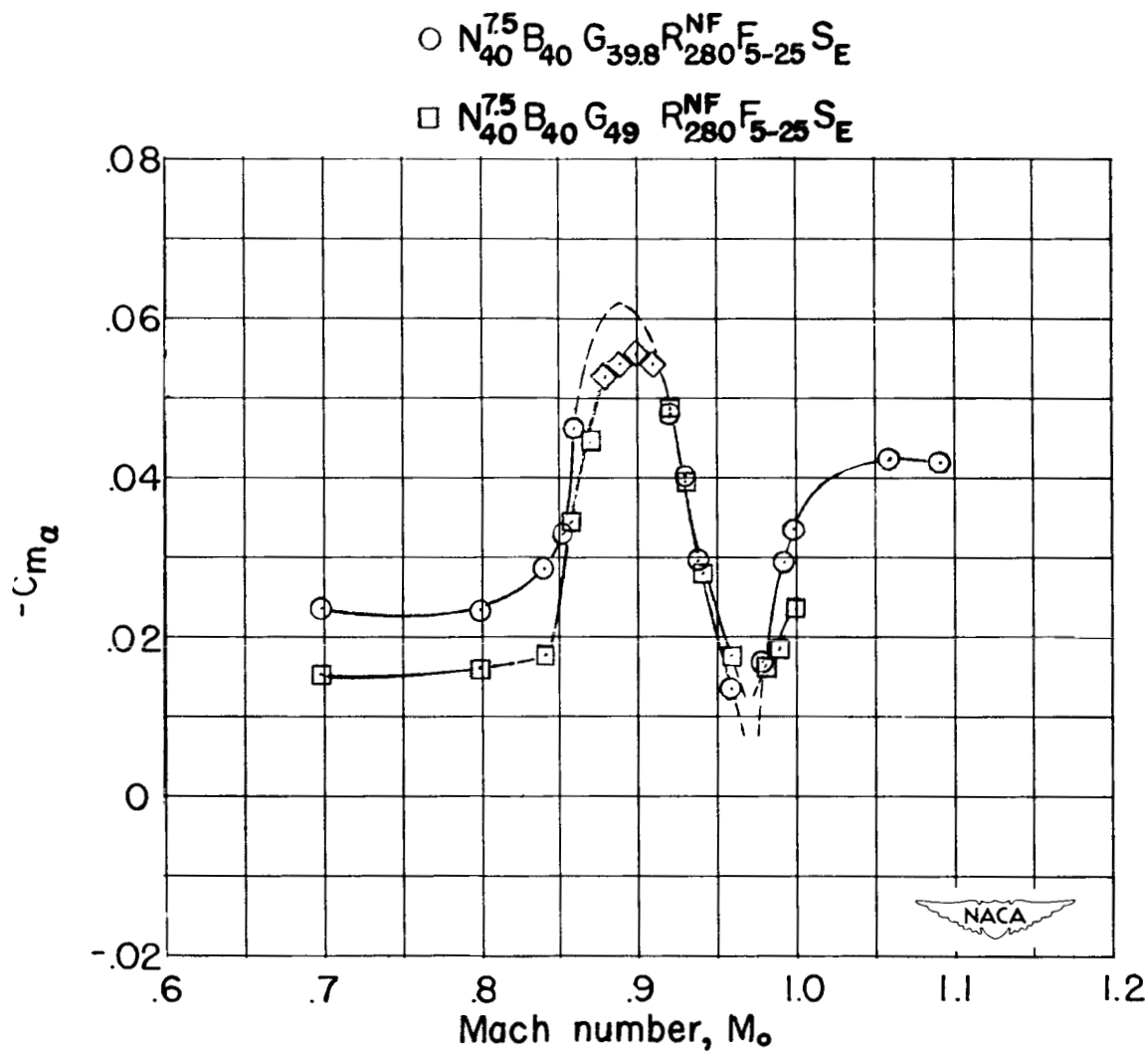
DECLASSIFIED



(a) Dynamic stability.

Figure 11.- The effects of changes in center-of-gravity location on the stability characteristics of the Mark-6.

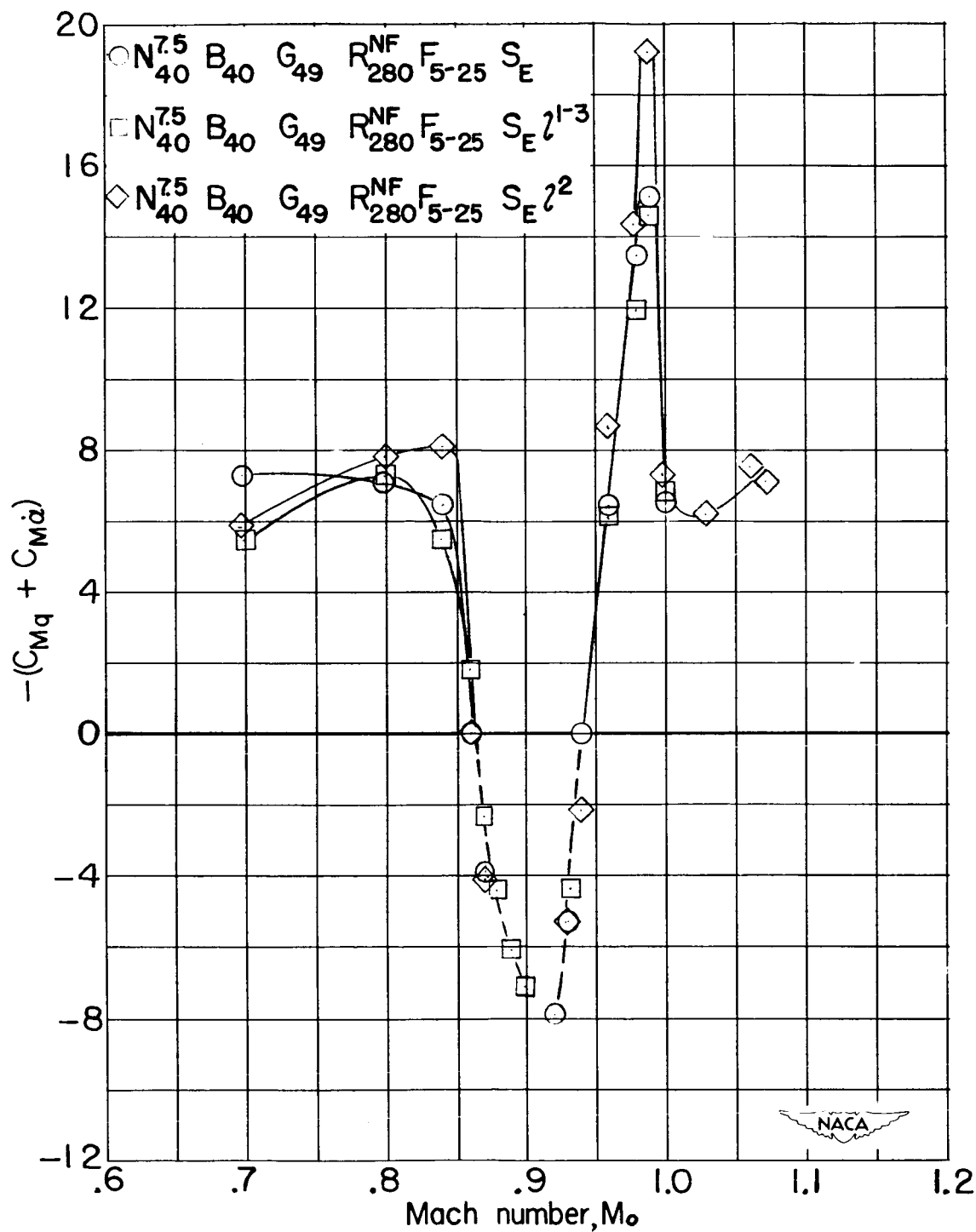
DECLASSIFIED



(b) Static stability.

Figure 11.- Concluded.

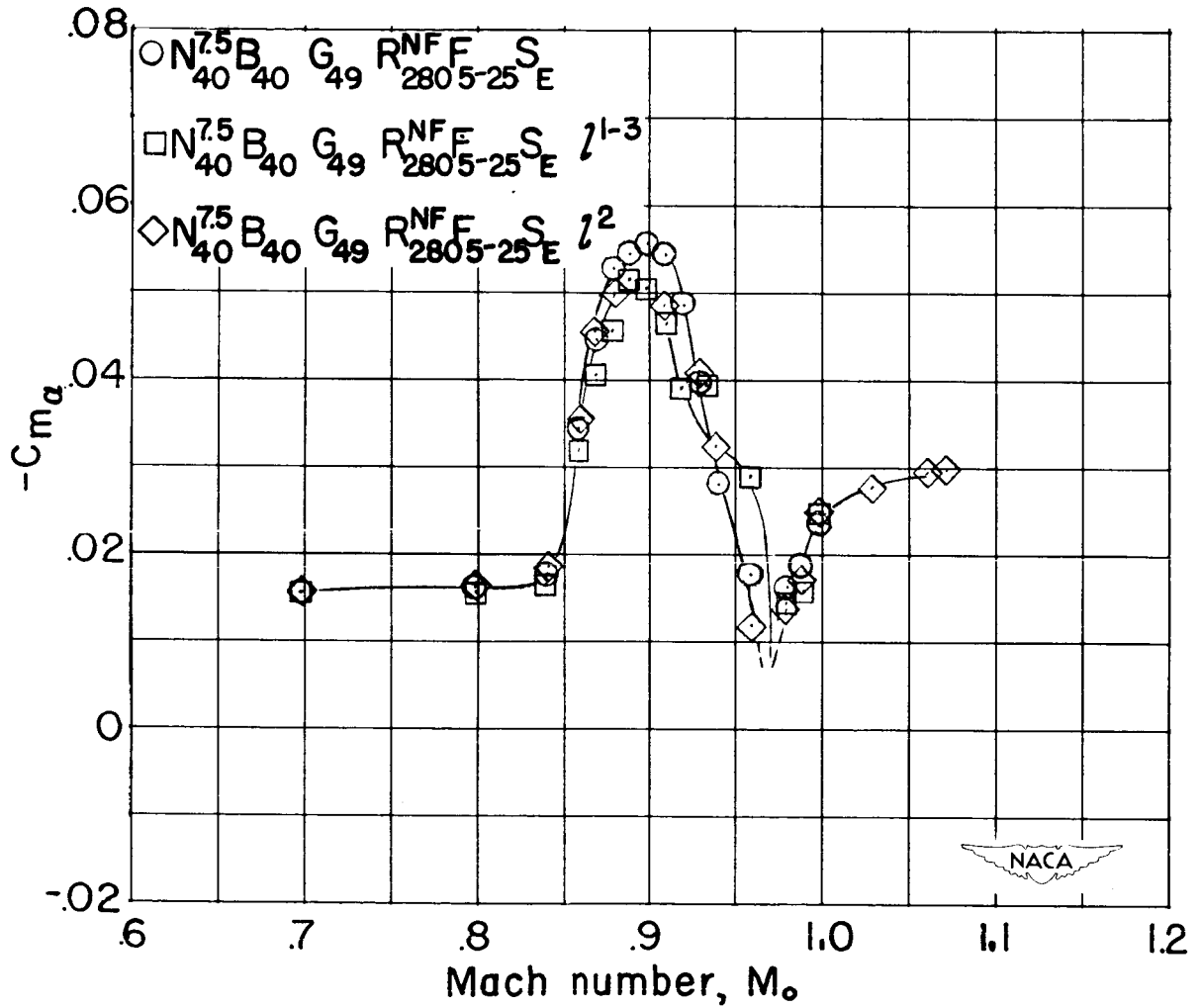
DECLASSIFIED



(a) Dynamic stability.

Figure 12.- The effects of the addition of suspension lugs on the stability characteristics of the Mark-6.

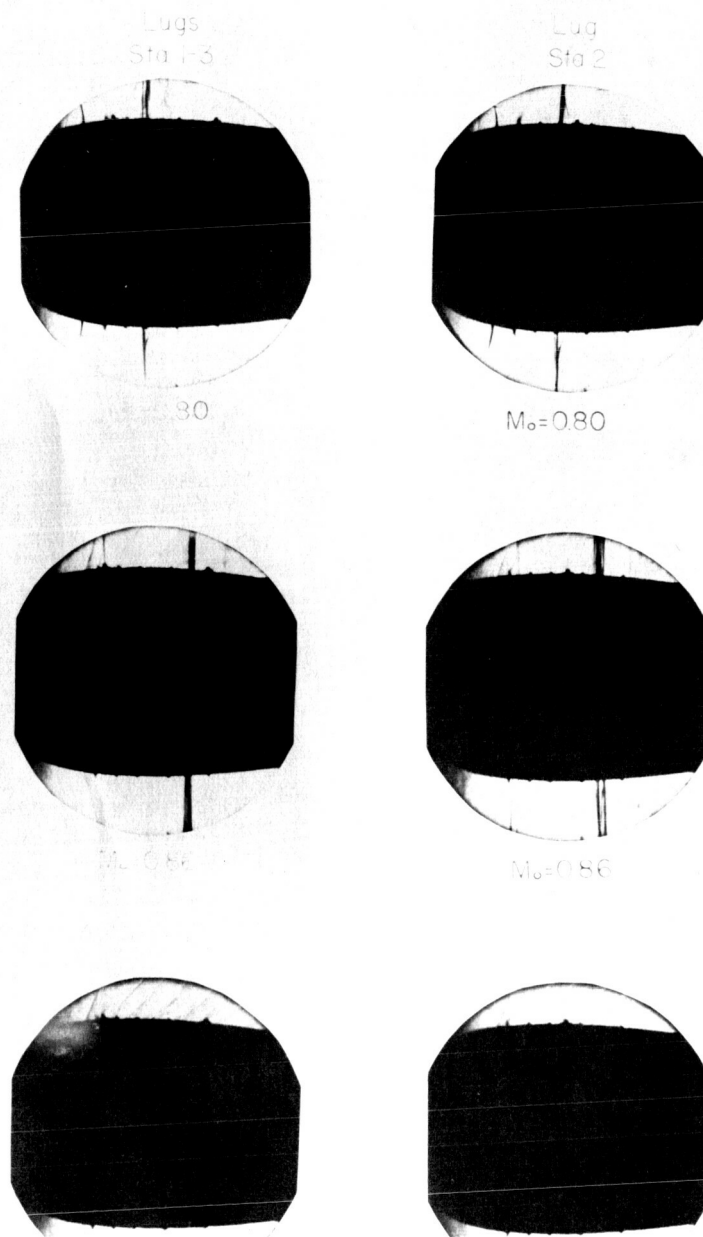
DECLASSIFIED



(b) Static stability.

Figure 12.- Continued.

DECLASSIFIED



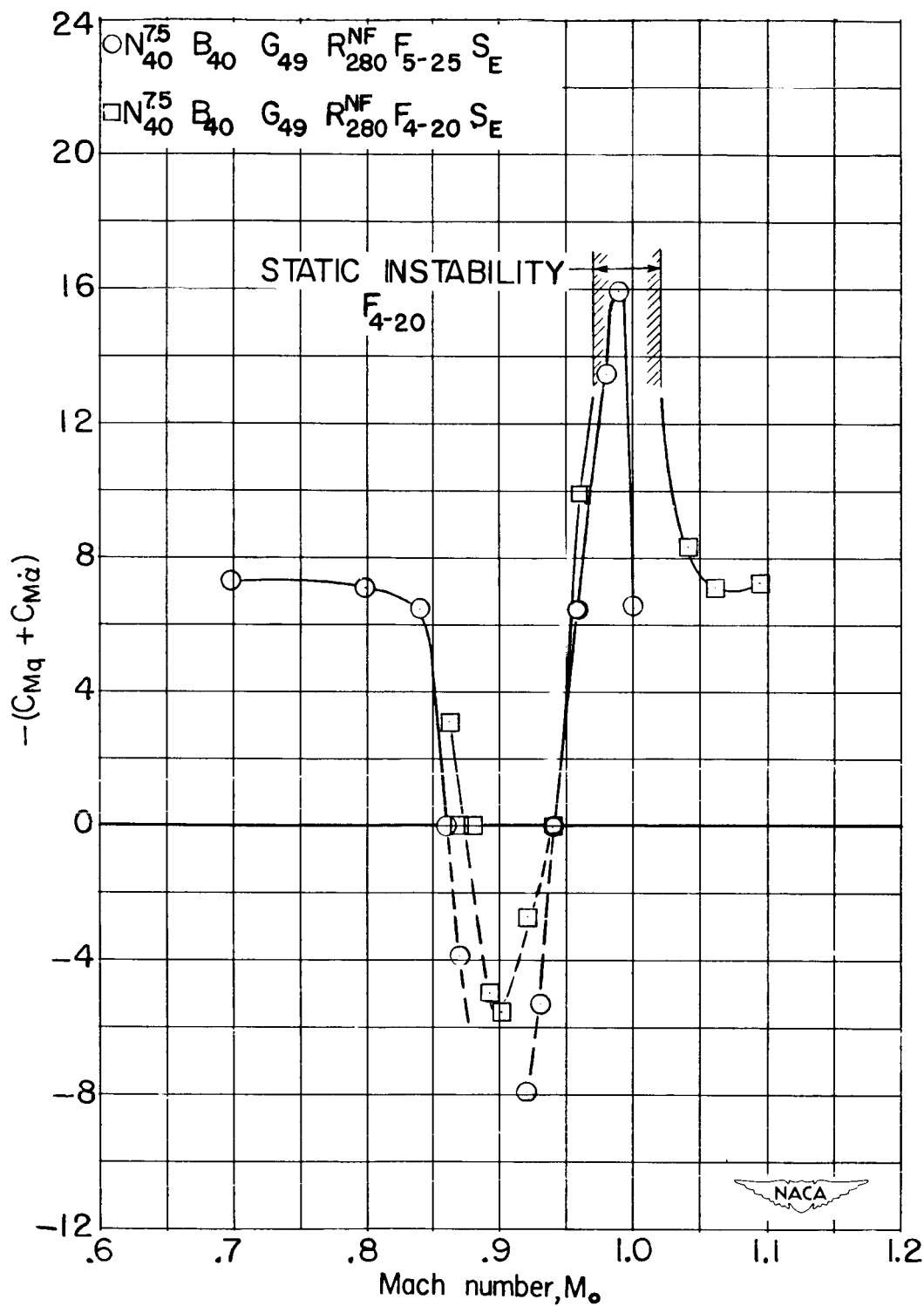
(c) Schlieren photographs.

Figure 12.- Concluded.



RDP No. 251

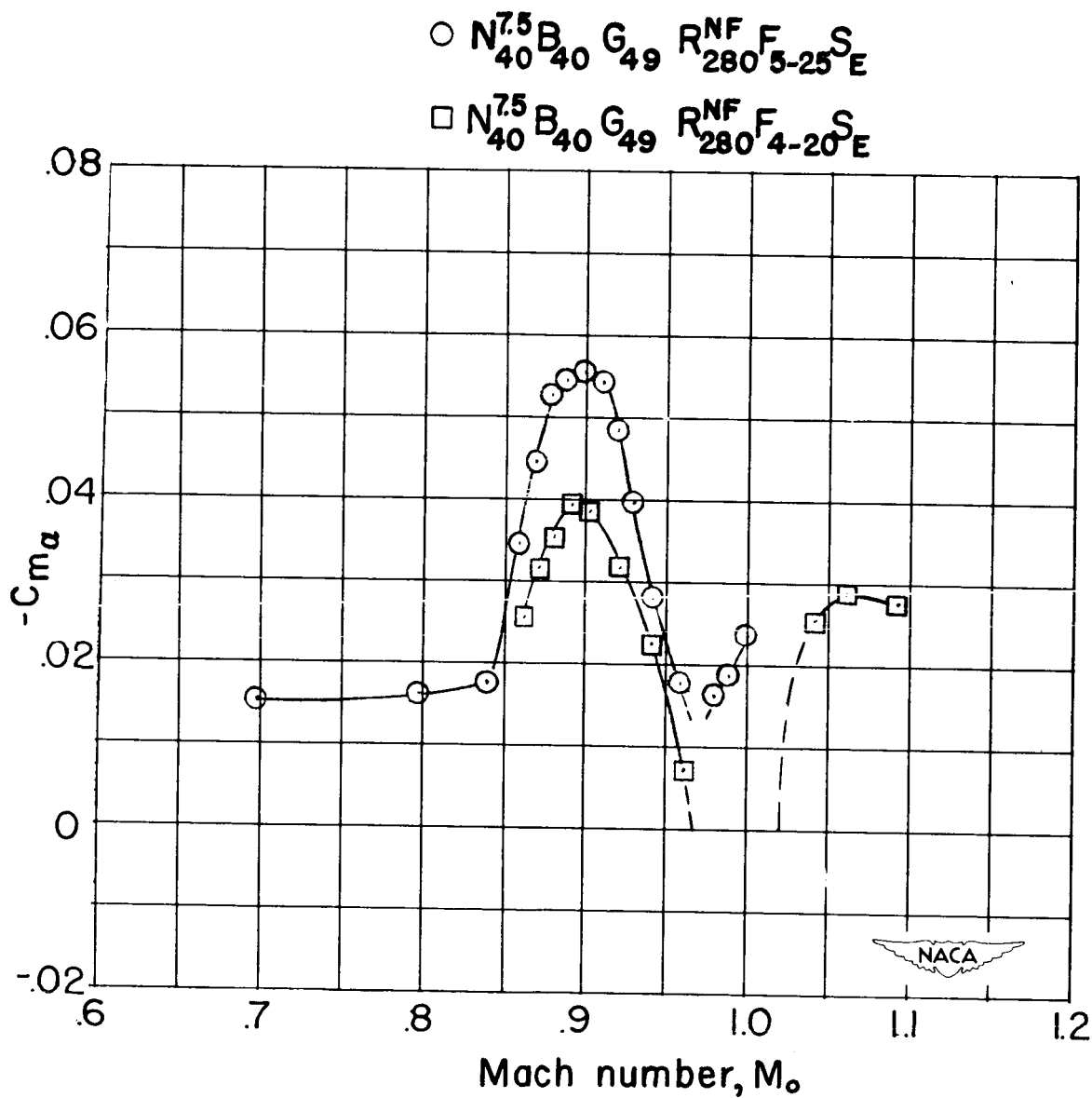
DECLASSIFIED



(a) Dynamic stability.

Figure 13.- The effects of the use of 4°-20° fins on the stability characteristics of the Mark-6.

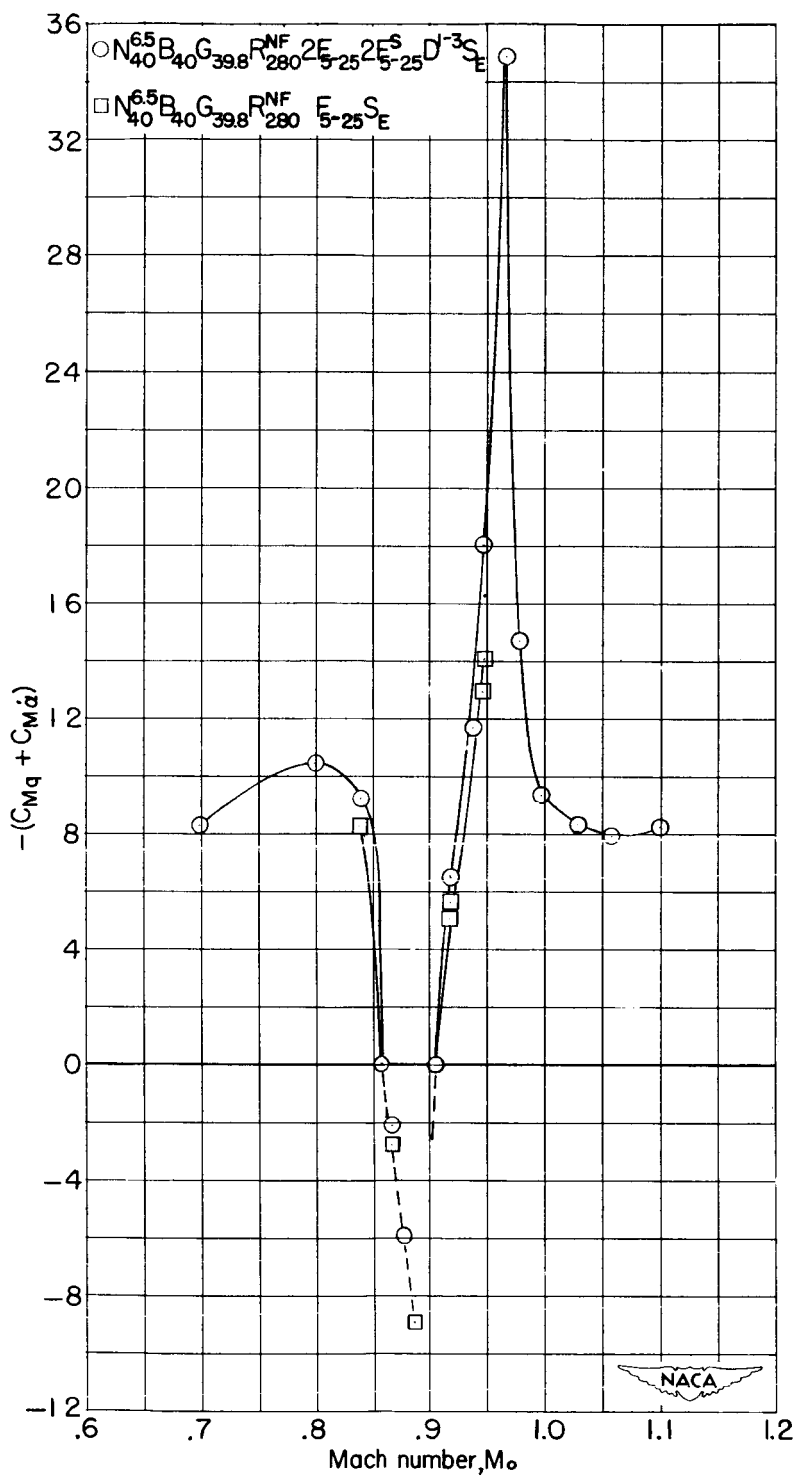
DECLASSIFIED



(b) Static stability.

Figure 13.- Concluded.

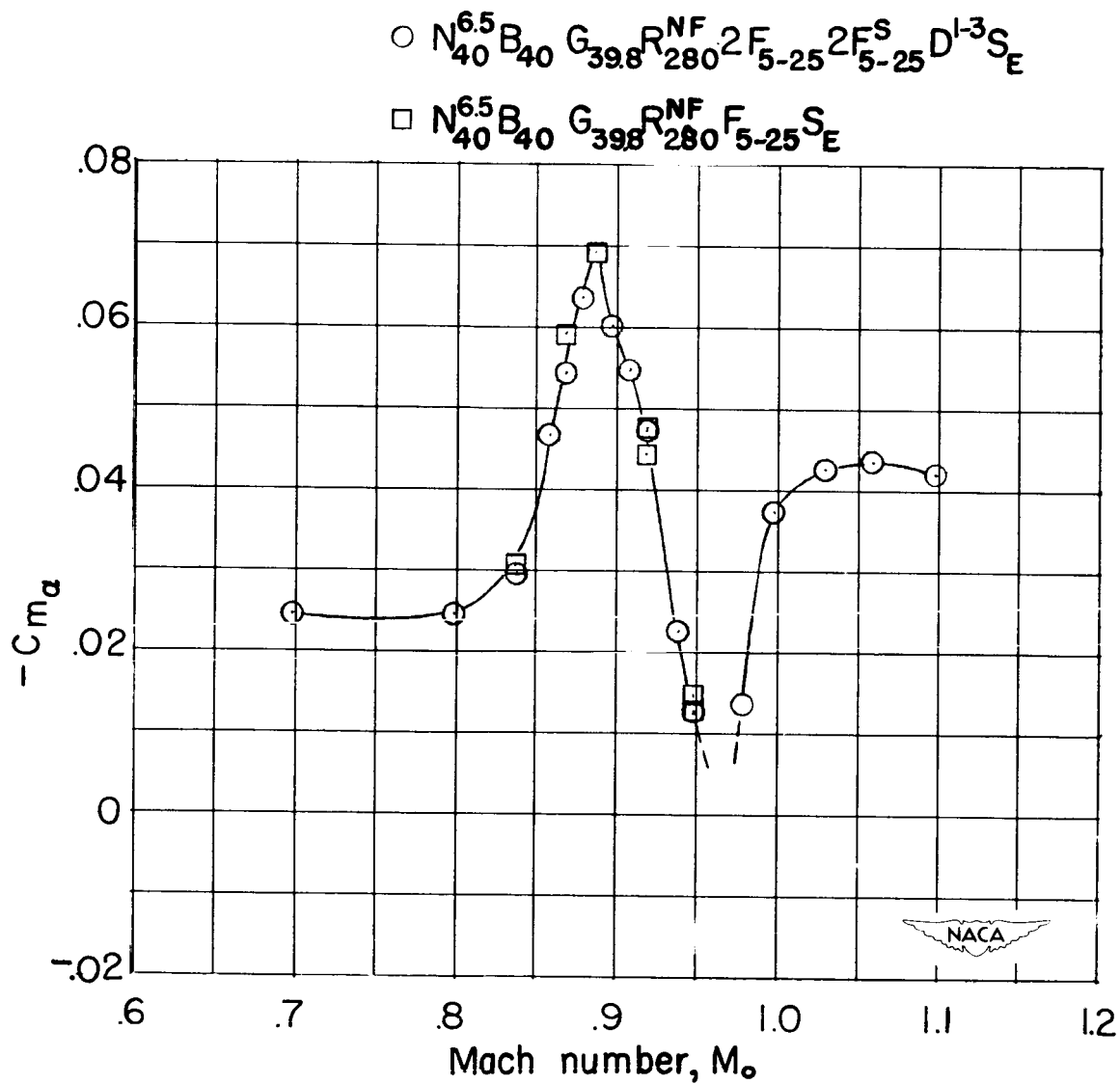
DECLASSIFIED



(a) Dynamic stability.

Figure 14.- The effects of the addition of fin-mounted fan ducts on the stability characteristics of the Mark-6.

DECLASSIFIED

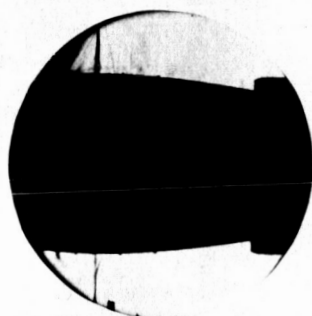


(b) Static stability.

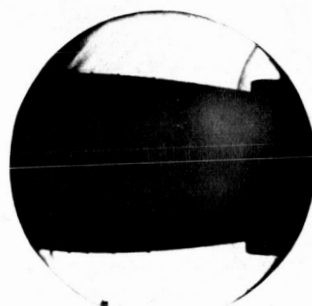
Figure 14.- Continued.

DECLASSIFIED

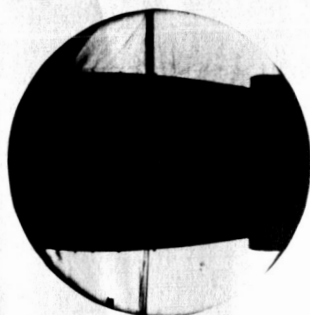
Mark 6



$M_o=0.80$



$M_o=0.97$



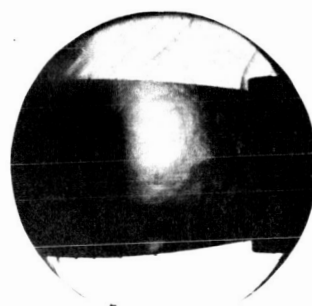
$M_o=0.87$



$M_o=1.06$



$M_o=0.94$



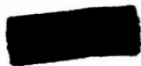
$M_o=1.105$

(c) Schlieren photographs.

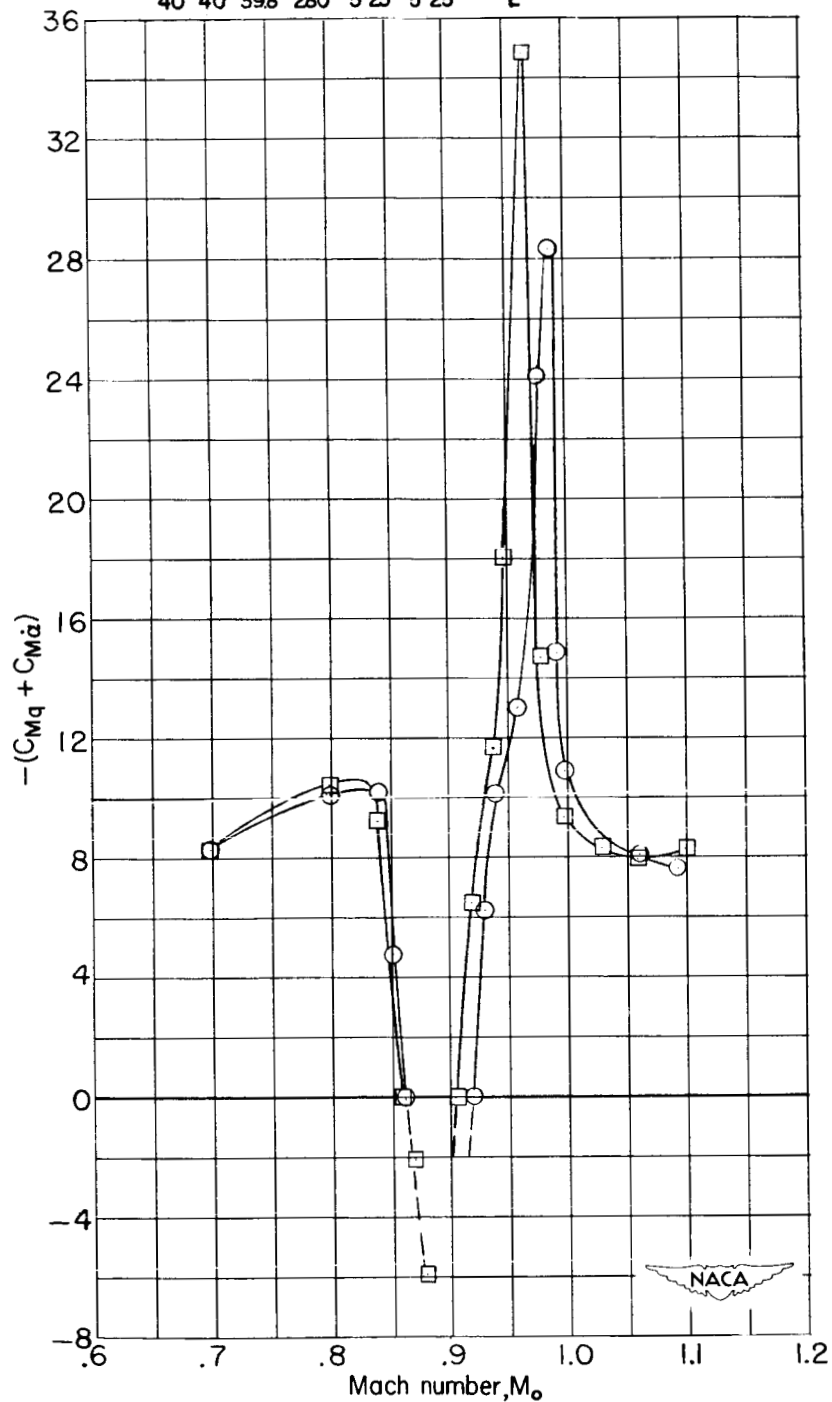
Figure 14.- Concluded.



RDP No.252

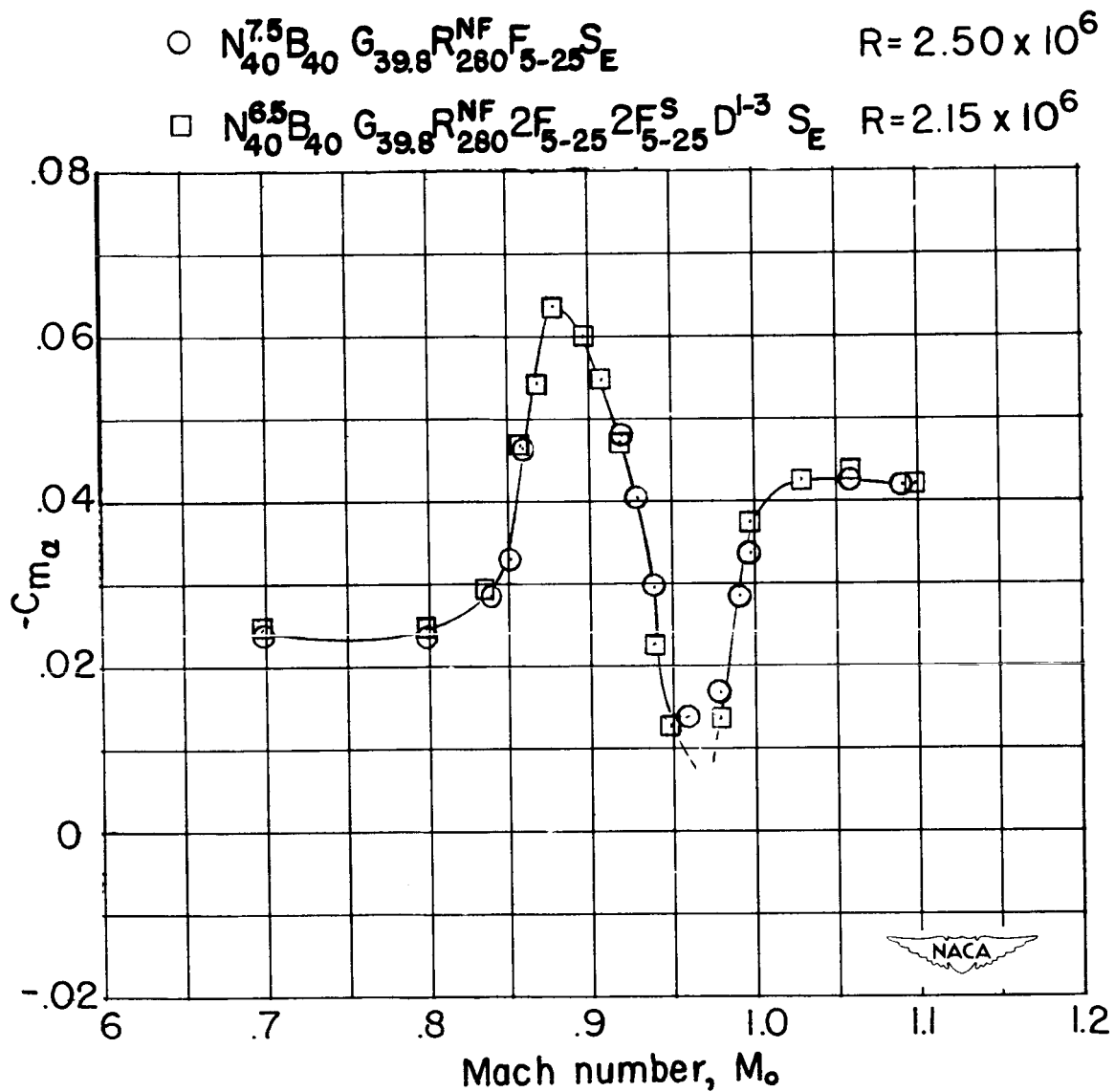


\circ N₇₅B₄₀G₄₀R₃₉₈^{NF}E₂₈₀S₅₋₂₅E R=2.50x10⁶
 \square N₆₅B₄₀G₄₀R₃₉₈^{NF}2E₂₈₀2E₅₋₂₅⁹D₅₋₂₅³S_E R=2.15x10⁶



(a) Dynamic stability.

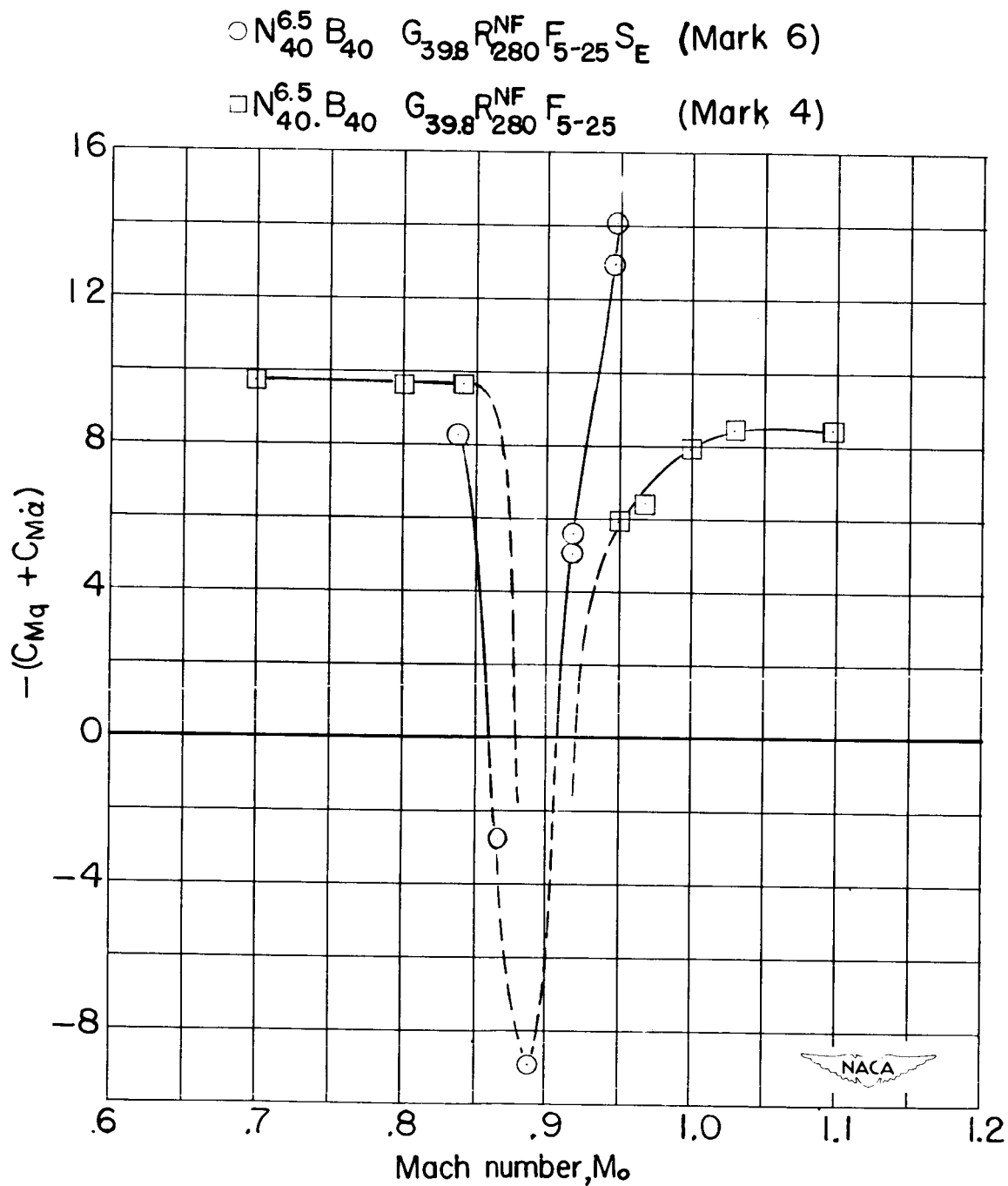
Figure 15.- The effects of the addition of fin-mounted fan ducts and a change in Reynolds number on the stability characteristics of the Mark-6.



(b) Static stability.

Figure 15.- Concluded.

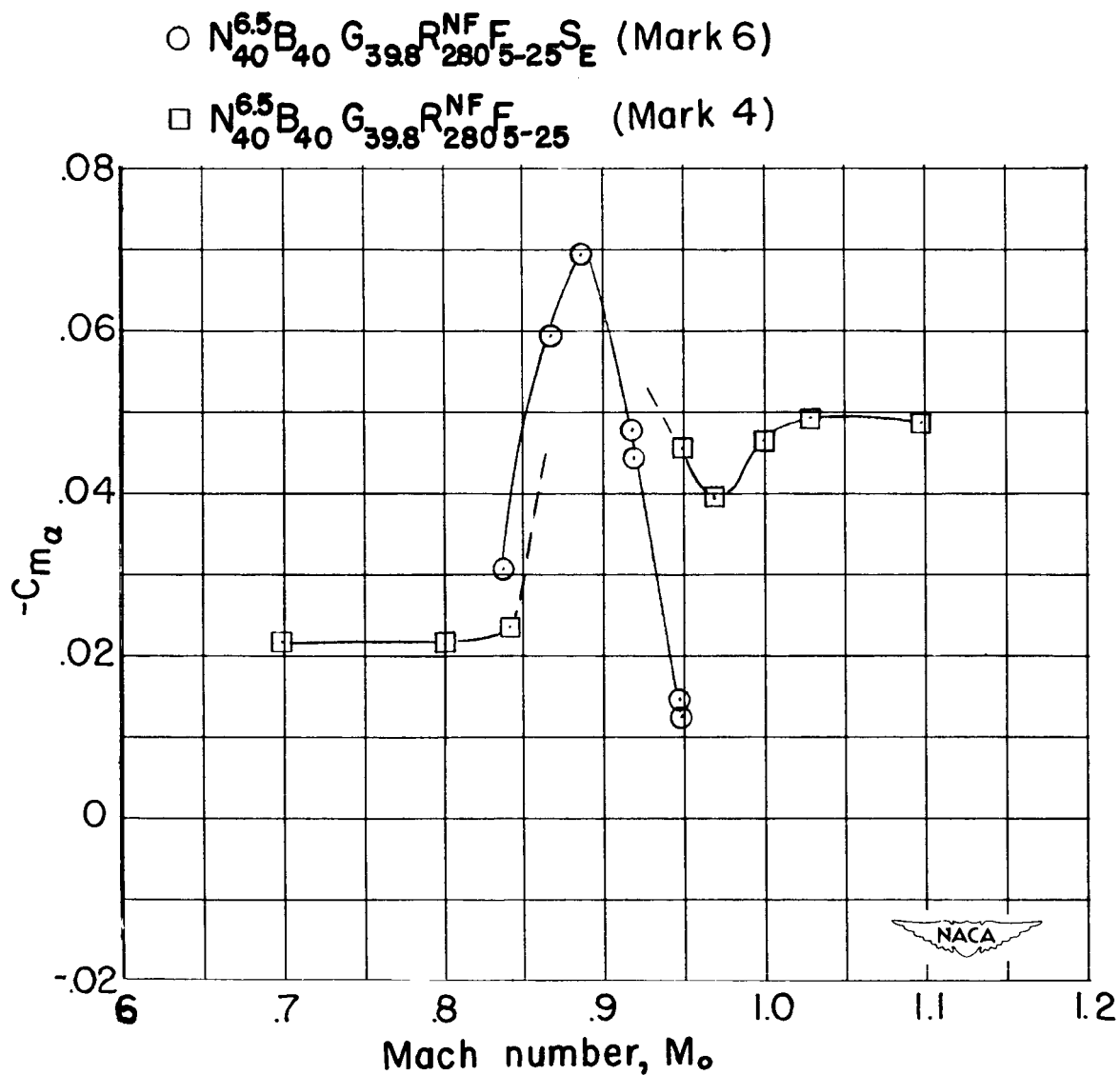
DECLASSIFIED



(a) Dynamic stability.

Figure 16.- The stability characteristics of the Mark-4 configuration.

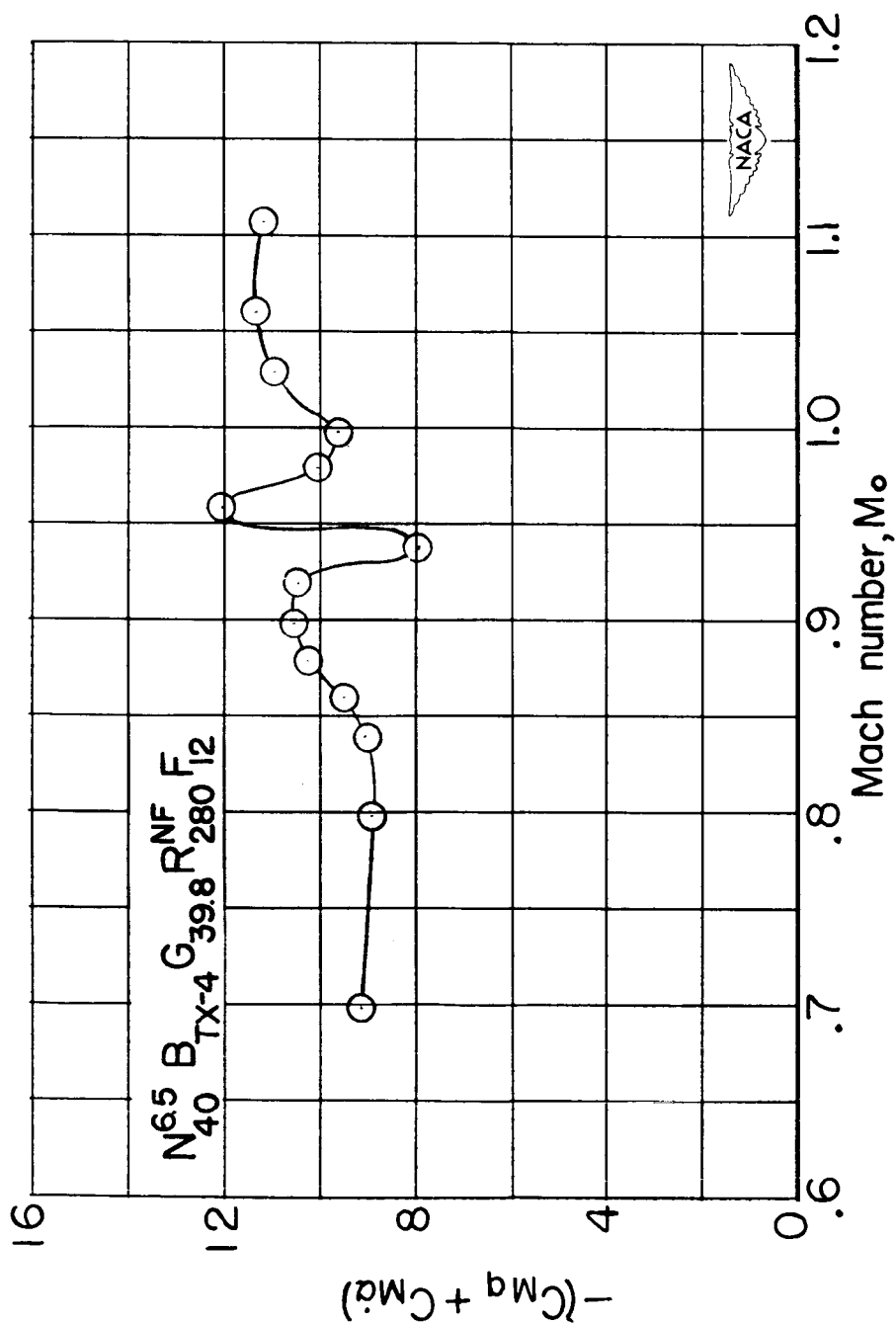
DECLASSIFIED



(b) Static stability.

Figure 16.- Concluded.

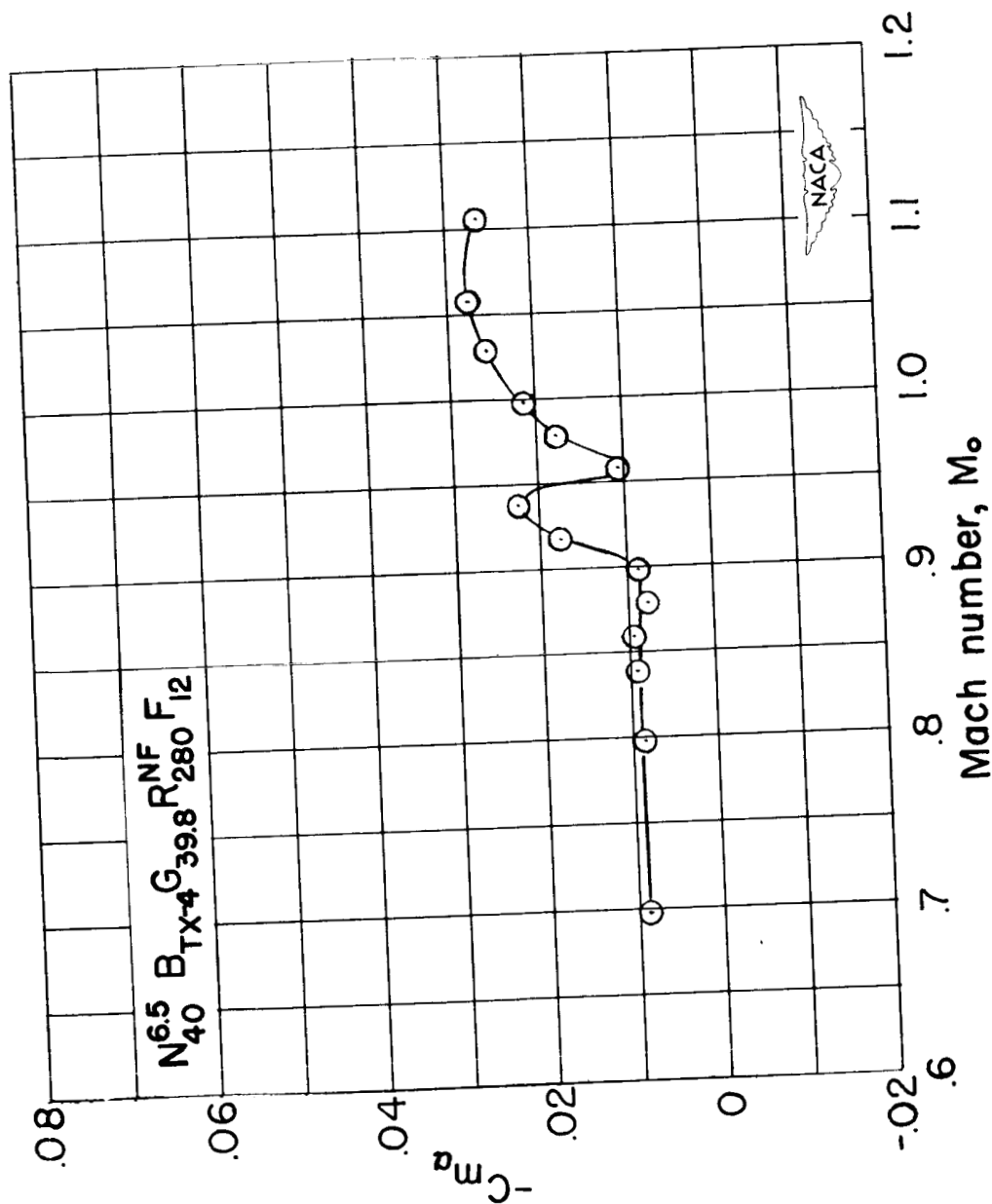
DECLASSIFIED



(a.) Dynamic stability.

Figure 17.- The stability characteristics of the TX-4 configuration.

DECLASSIFIED

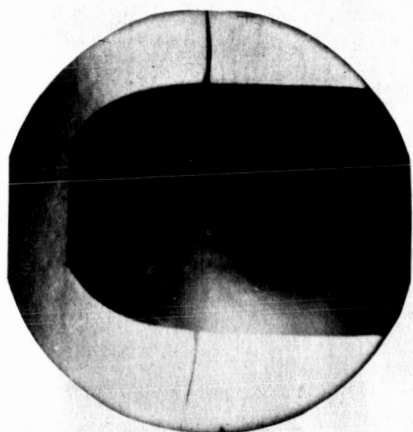


(b) Static stability.

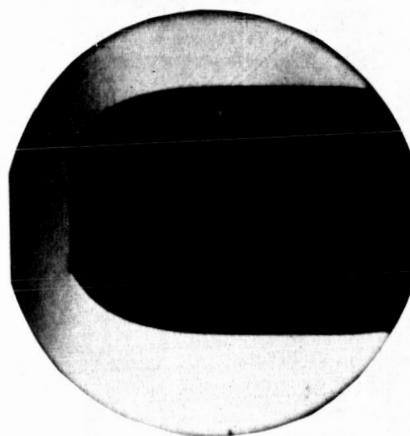
Figure 17.- Continued.

DECLASSIFIED

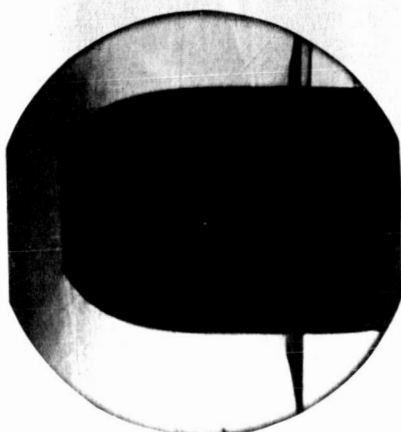
TX-4



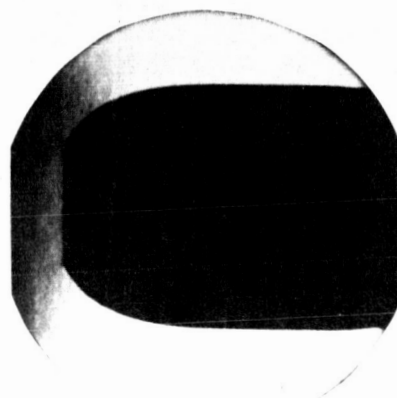
$M_o=0.80$



$M_o=0.98$



$M_o=0.88$



$M_o=1.06$

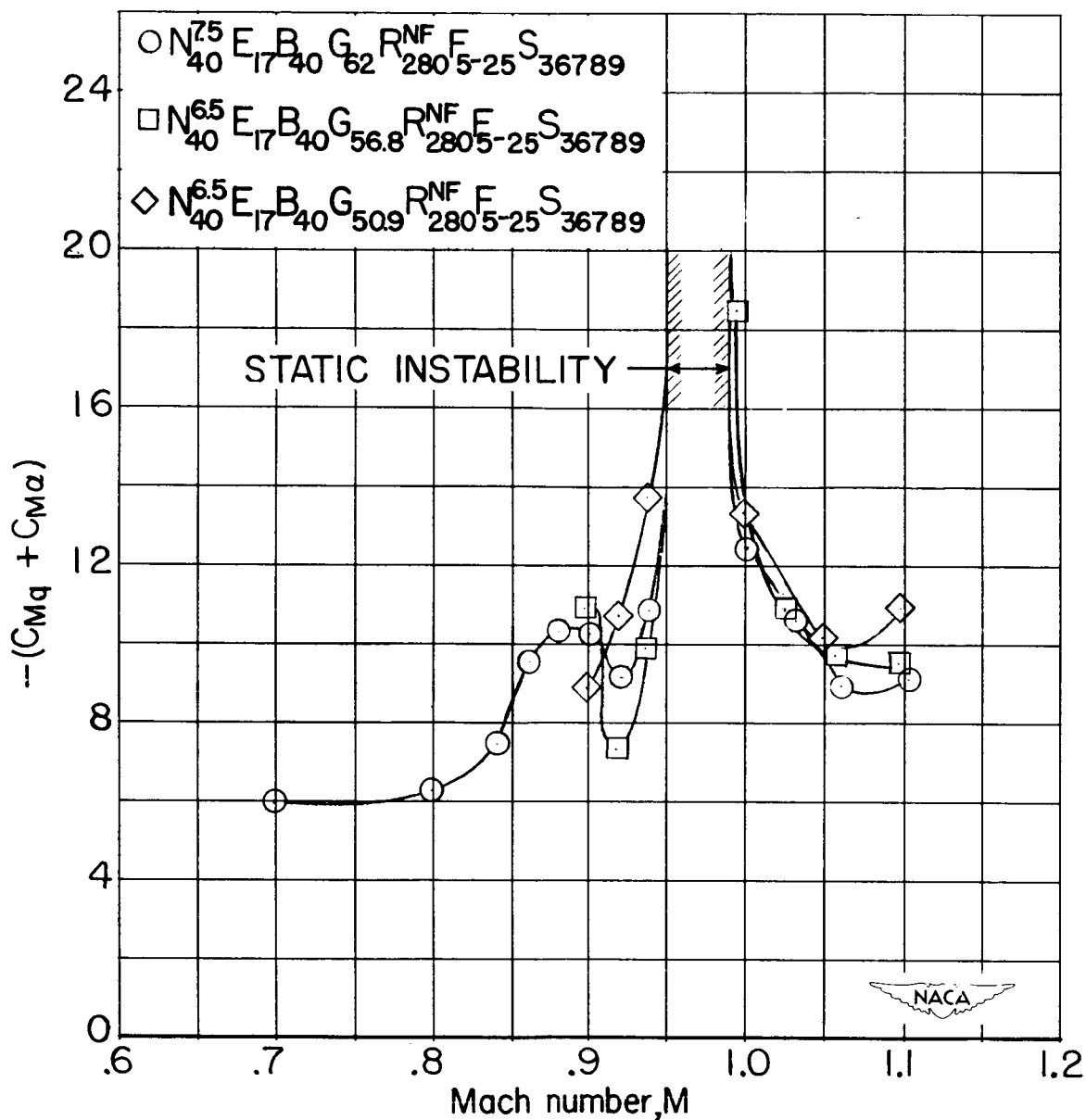
(c) Schlieren photographs.

Figure 17.- Concluded.



RDP No. 253

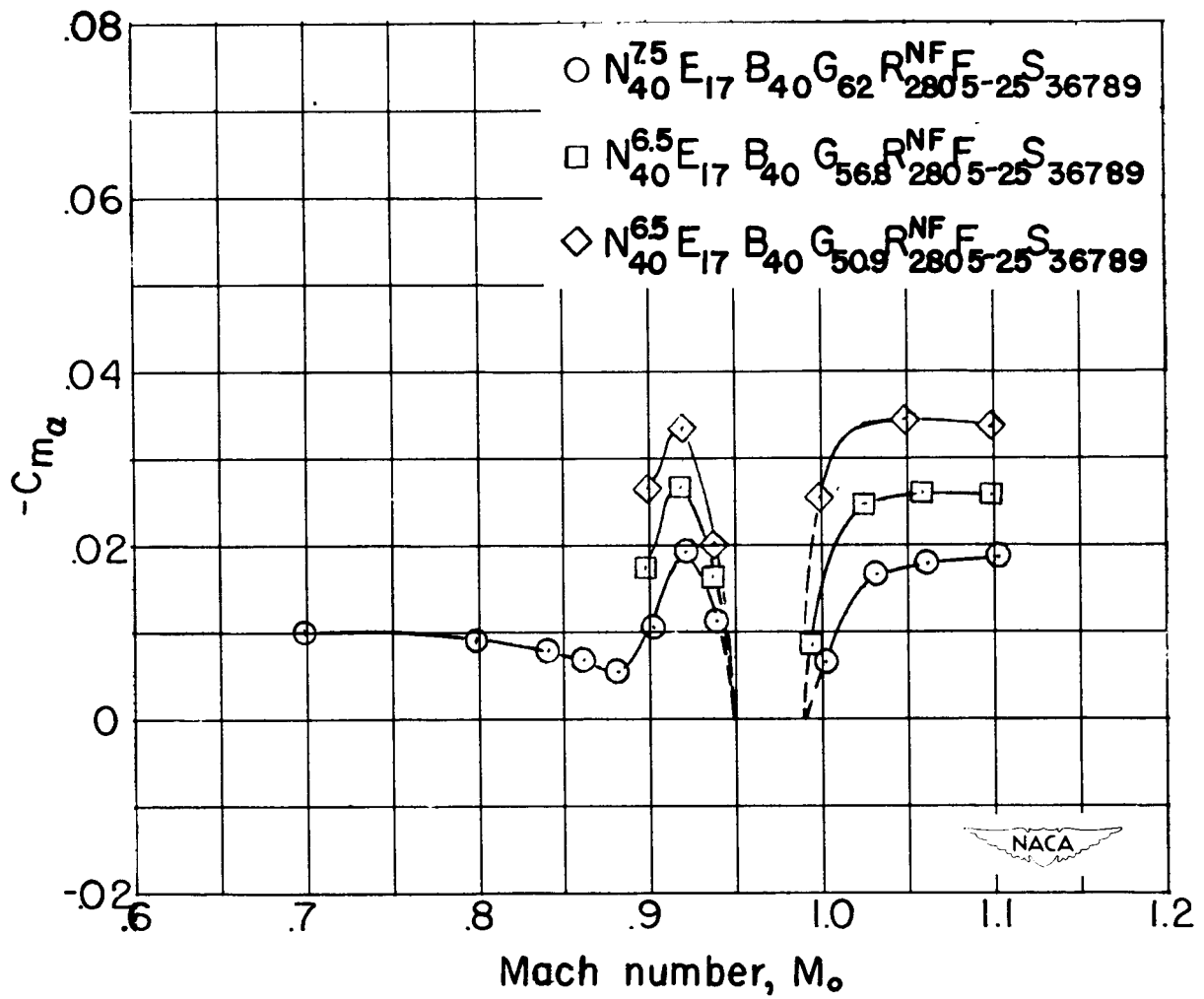
DECLASSIFIED



(a) Dynamic stability.

Figure 18.- The stability characteristics of the TX-13B' and the effects of changes in center-of-gravity location.

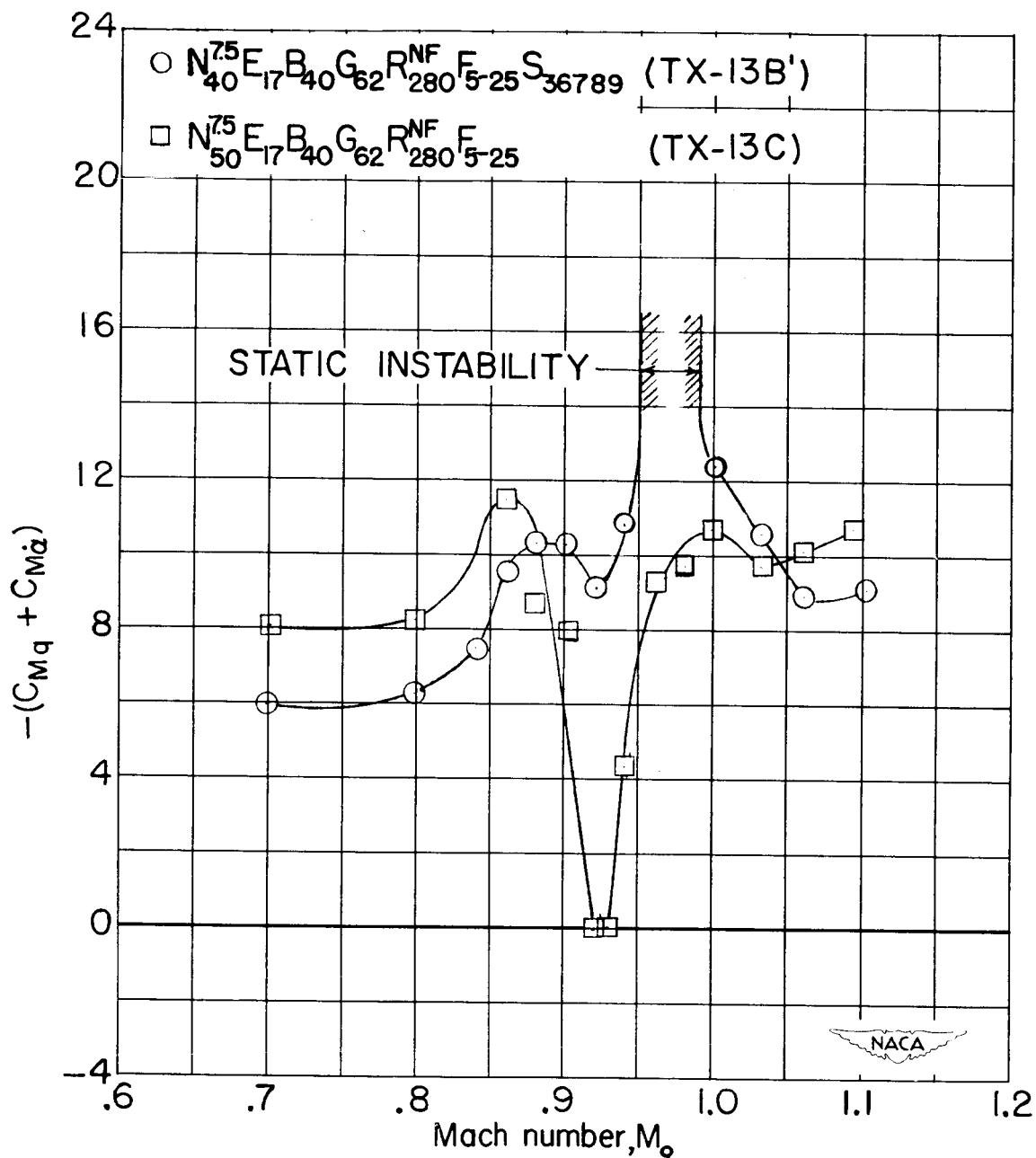
SECRET



(b) Static stability.

Figure 18.- Concluded.

DECLASSIFIED

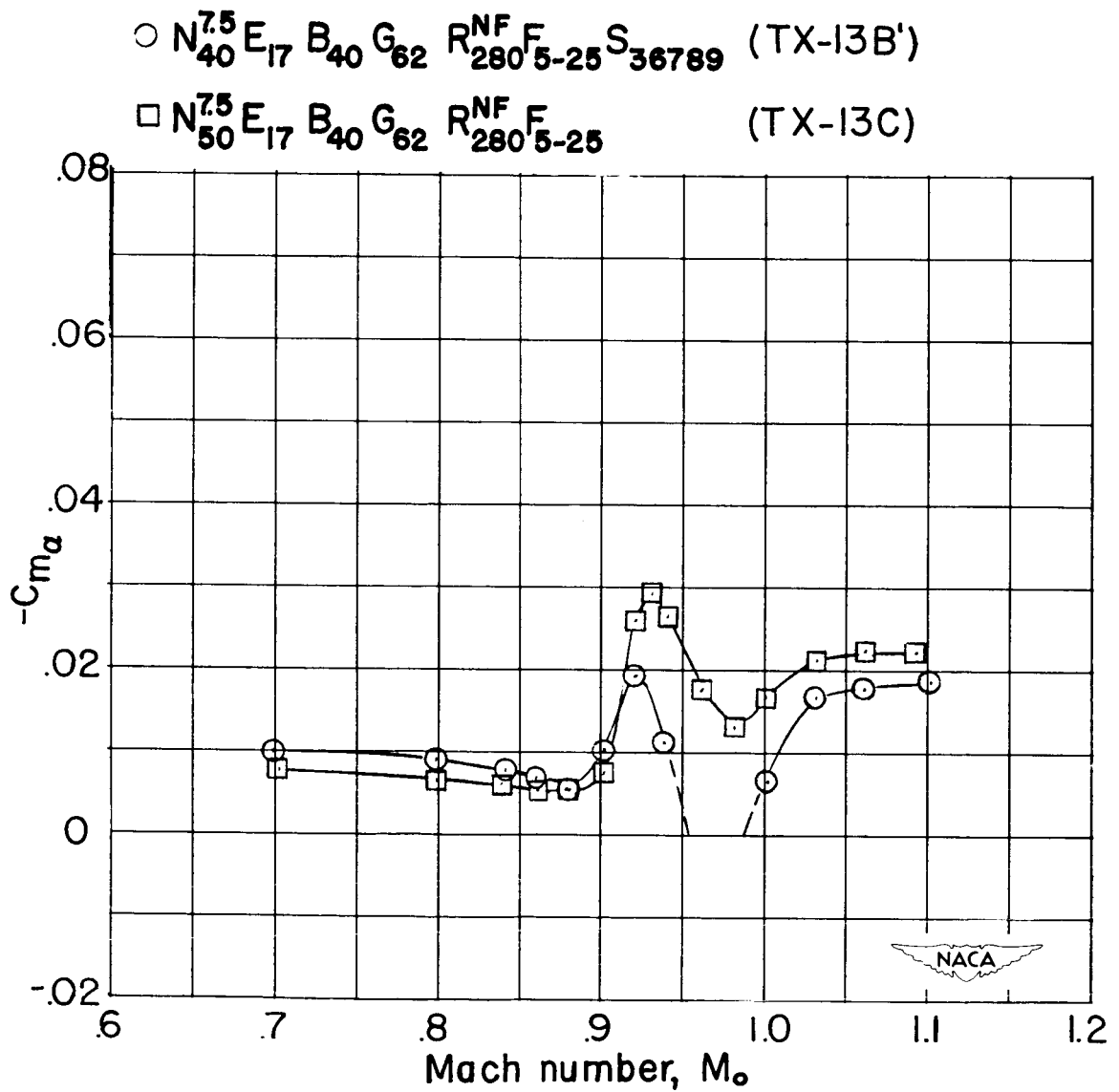


(a) Dynamic stability.

Figure 19.- The stability characteristics of the TX-13B' and the TX-13C configurations.

DECLASSIFIED

NACA RM SL53G09c

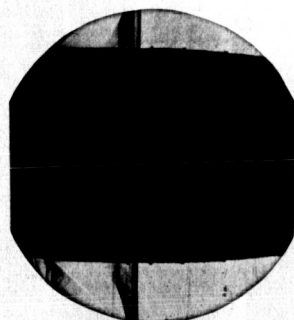


(b) Static stability.

Figure 19.- Continued.

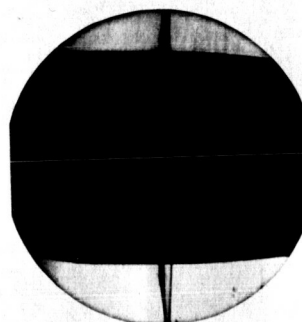
DECLASSIFIED

TX-13B'

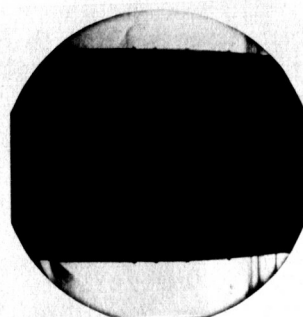


$M_o=0.86$

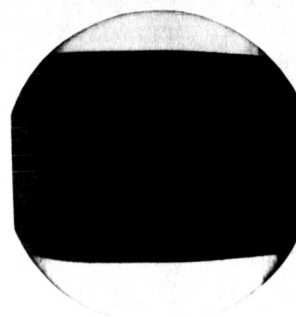
TX-13C



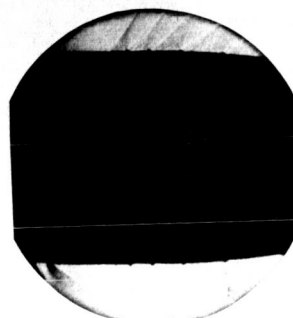
$M_o=0.86$



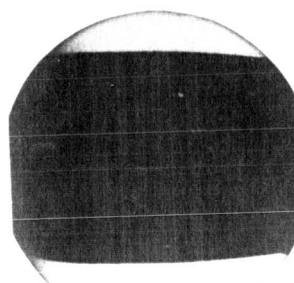
$M_o=0.92$



$M_o=0.92$



$M_o=1.00$



$M_o=1.00$

(c) Schlieren photographs.

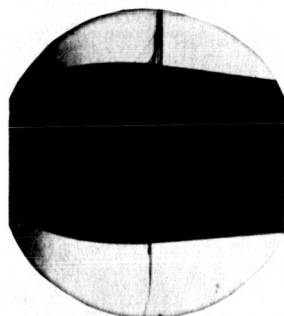
Figure 19.- Concluded.



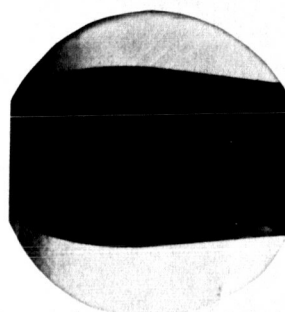
RDP No. 254

DECLASSIFIED

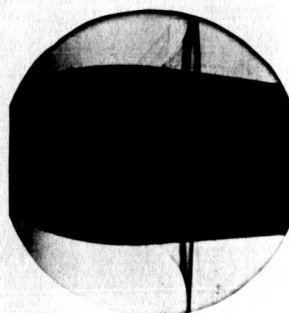
Mark 5



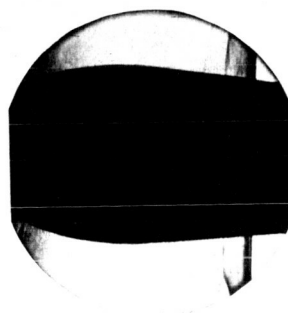
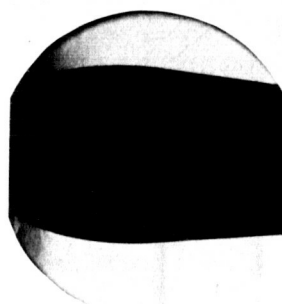
$M_o=0.84$



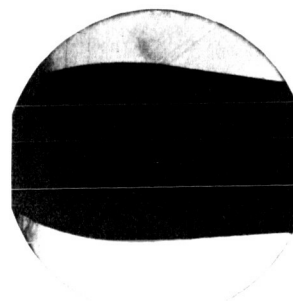
$M_o=0.98$



$M_o=0.88$



$M_o=0.92$



$M_o=1.10$

(c) Schlieren photographs.



Figure 20.- Concluded.

RDP No.255